Transp Porous Med (2011) 89:185–212
DOI 10.1007/s11242-011-9764-3

Effects of Chemical Reaction, Heat, and Mass Transfer on Non-Newtonian Fluid Flow Through Porous Medium in a Vertical Peristaltic Tube

M. F. El-Sayed · N. T. M. Eldabe · A. Y. Ghaly · H. M. Sayed

Received: 9 September 2009 / Accepted: 6 April 2011 / Published online: 20 April 2011

Abstract The effect of mass diffusion of chemical species with first-order reaction on peristaltic motion of an incompressible Jeffrey fluid has been investigated. The fluid flows through vertical porous media in the gap between concentric tubes with heat and mass transfer. The inner tube is uniform, while the outer one is a non-uniform tube has a sinusoidal wave traveling down its wall. A perturbation solution, under long-wavelength assumption, is obtained which satisfies the momentum, energy, and concentration equations for the case of small porosity parameter. Numerical results for the behaviors of pressure rise and frictional force per wavelength as well as for the skin friction, Nusselt number, and Sherwood number with other physical parameters are obtained. Several graphs for these results of physical interest are displayed and discussed in detail.

Keywords Peristaltic transport · Chemical reaction · Heat and mass transfer · Non-Newtonian fluids · Flows through porous media

1 Introduction

Peristaltic transport is a form of fluid transport generated by a progressive wave of area contraction or expansion along the length of a distensible tube containing fluid. Peristalsis induces in general propulsive and mixing movements. Peristaltic pumping is found in many applications such as for the transport of slurries, sensitive or corrosive fluids, sanitary fluid, and noxious fluids in the nuclear industry, to name but a few examples. Extensive literature on the topic is available for viscous fluids (Hayat et al. 2008, 2009; Srinivas and Gayathri 2009;

M. F. El-Sayed · N. T. M. Eldabe · A. Y. Ghaly · H. M. Sayed
Department of Mathematics, Faculty of Education, Ain Shams University,
Heliopolis, Roxy, Cairo, Egypt

M. F. El-Sayed (✉)
Department of Mathematics, College of Science, Qassim University, P. O. Box 6644,
Buraidah 51452, Kingdom of Saudi Arabia
e-mail: mfahmye@yahoo.com

Srinivas and Kothandapani 2009). The theory of non-Newtonian fluids has received great attention during the recent years, because traditional viscous fluids cannot precisely describe the characteristics of many rheological fluids. The governing equations for such fluids are complicated and more nonlinear than the Navier–Stokes equations and present interesting challenges to physicists, computer scientists, mathematicians, and modelers.

Simultaneous heat and mass transfer from different geometries embedded in porous media has many engineering and geophysical applications such as geothermal reservoirs, drying of porous solids, thermal insulation, enhanced oil recovery, packed-bed catalytic reactors, cooling of nuclear reactors, and underground energy transport. Nakayama and Koyama (1987a,b) studied free convection over a vertical flat plate embedded in a thermally stratified porous medium. Gorla et al. (1996) have considered the effects of thermal dispersion and stratification on mixed convection about a vertical surface in a porous medium. Hassanien et al. (1998) studied the heat transfer characteristics of mixed convection flow over a vertical flat plate embedded in porous medium. The similarity solutions of hydromagnetic mixed convection heat and mass transfer for Hiemenz flow through porous media are explained by Chamkha and Khaled (2000). Recently, Liao and Pop (2004) offer a comprehensive account of the boundary layers over a vertical flat plate embedded in a porous medium.

In view of their importance, several authors have studied peristalsis in both mechanical and physiological situations. Abd El Naby and El Misery (2002) discussed the effect of an endoscope on the peristaltic mechanism of a generalized Newtonian fluid. El Misery et al. (2003) studied the peristaltic transport of a fluid with variable viscosity through the gap between concentric uniform tubes. Hayat et al. (2006) investigated the peristaltic flow of a Jeffrey fluid through the gap between concentric uniform tubes. Hayat et al. (2008) explained the influence of an endoscope on the peristaltic flow of a Jeffrey fluid through tubes. The interaction of peristalsis and heat transfer has also received some attention as it might be relevant in processes like hemodialysis and oxygenation. Radhakrishnamacharya and Radhakrishnamurty (1993) investigated peristalsis with heat transfer in a non-uniform channel. Radhakrishnamacharya and Srinivasulu (2007) explained the effect of elasticity of the flexible walls on peristaltic transport of an incompressible viscous fluid, with heat transfer. Vajravelu et al. (2007) studied the interaction of peristalsis with heat transfer for the flow of a viscous fluid in a vertical porous annular region between two concentric tubes.

On the other hand, the analysis of blood flow through tapered tubes is very important to understand the behavior of the flow as the taper of the tube is an important factor in the pressure development. It has been pointed out that the blood vessels bifurcate at frequent intervals and although the individual segments of arteries may be treated as uniform between bifurcations, the diameter of the artery decreases quite fast at each bifurcation (Dwivedi et al. 1982). It has been observed that even for the small angles of taper (up to 2), the effects of tapering of the blood vessels cannot be neglected (Chaturani and Pralhad 1985). As pointed out by How and Black (1987), this study is also very useful for the design of prosthetic blood vessels as the use of grafts of tapered lumen has the advantage of surgical benefits, the blood vessels being wider upstream. The important hydrodynamic factor for tapered tube geometry is the pressure loss which leads to the diminished blood flow through the grafts. It has been pointed out that in some diseased conditions, e.g., patients with sever myocardial infarction, cerebrovascular diseases, and hypertension, blood exhibits remarkable non-Newtonian properties (Chien 1981; Chaturani and Samy 1985). Hence, it is appropriate to model blood as a non-Newtonian fluid when it flows through narrow arteries at low-shear rates (Sankar and Hemalatha 2006, 2007a,b,c). Gupta and Seshadri (1976) analyzed the peristaltic flow through non-uniform channels and tubes with reference to the flow of spermatic fluid in vas deferens, neglecting the inertia terms (considering them to be small in comparison to the viscous terms). Srivastava and Srivastava (1982) extended the analysis to that of a two-layer model. Deshikachar and Rao (1985) studied the effect of a magnetic field on the flow and oxygenation of an incompressible Newtonian conducting fluid in channels with irregular boundaries. Rao and Deshikachar (1986) investigated the effect of unsteadiness on magnetohydrodynamic (MHD) flow of a conducting incompressible viscous fluid in channels of varying cross section. Misra and Pandey (1995) put forward a theoretical analysis for the axisymmetric peristaltic motion of a Newtonian viscous incompressible fluid through a flexible tube of changing cross section, where the nonlinear convective acceleration terms are not negligible compared to the viscous terms. Elshehawey et al. (1998) studied the peristaltic motion of Carreau fluid in a non-uniform channel. Mekheimer (2004) studied the effect of a uniform magnetic field on peristaltic transport of a blood, represented by a couple-stress fluid, in a non-uniform two-dimensional channels. Also, Elshehawey et al. (2005) studied the axisymmetric peristaltic motion of a viscous compressible liquid through a flexible pore of variable cross section. Mekheimer (2005) studied the peristaltic transport of a viscous incompressible fluid (creeping flow) through the gap between coaxial tubes. Eldabe et al. (2007) investigated the peristaltic pumping of MHD non-Newtonian biviscosity fluid through an axisymmetric non-uniform tube in the presence of a radial magnetic field.

In this article, a mathematical model is presented to study the effects of chemical reaction on the interaction among peristalsis, heat, and mass transfer for the motion of a non-Newtonian Jeffrey fluid embedded in a vertical porous medium in two-dimensional tubes. The outer tube is non-uniform and has a sinusoidal wave traveling down its wall, and the inner one is a rigid, uniform tube. This problem, to the best of our knowledge, has not been investigated yet. The momentum, energy, and mass equations have been linearized under long-wavelength assumptions, and analytical solutions for the flow variables have been obtained. Numerical results for the behaviors of pressure rise and frictional force per wavelength as well as for the skin friction, Nusselt number, and Sherwood number with other physical parameters are obtained. Several graphs for these results of physical interest are displayed and discussed in detail.

2 Formulation of the Problem

Consider the flow of an incompressible Jeffrey fluid through porous medium in the gap between two coaxial vertical tubes. The influences of chemical reaction, heat, and mass transfer are taken into account. The outer tube is non-uniform and has a sinusoidal wave traveling down its wall, and the inner one is a rigid, uniform tube. We choose a rectangular coordinate system for the tubes with $\bar{x}$ along the center line of the inner and the outer tubes, $\bar{y}$ is the radial distance measured, the inner tube is at $\bar{y} = \bar{y}_1$ and kept at a temperature T_i and concentration C_i, and the outer tube is at $\bar{y} = \bar{y}_2$ and kept at a temperature T_o and concentration C_o. The geometry of the two wall surfaces, see Fig. 1, are

$$\bar{y}_1 = a_\mathrm{i} \quad \text{and} \quad \bar{y}_2 = a_0 + b\sin[\tfrac{2\pi}{\lambda}(\bar{x} - c\bar{t})] \tag{1}$$

in which a_i signifies the radius of the inner tube, a_0 indicates the radius of the outer tube at the inlet, c is the wave speed, $\bar{t}$ is the time, b is the amplitude, and λ is the wavelength. The radius of the tapered tube is given by Sankar and Hemalatha (2007c)

$$a_0(\bar{x}) = R - \bar{x}\tan\psi \tag{2}$$

where R is the radius at $\bar{x} = 0$, ψ is the angle of taper which is considered as a constant in this study (the case of convergent tube $\psi = \text{constant}$).

Fig. 1 Flow configuration

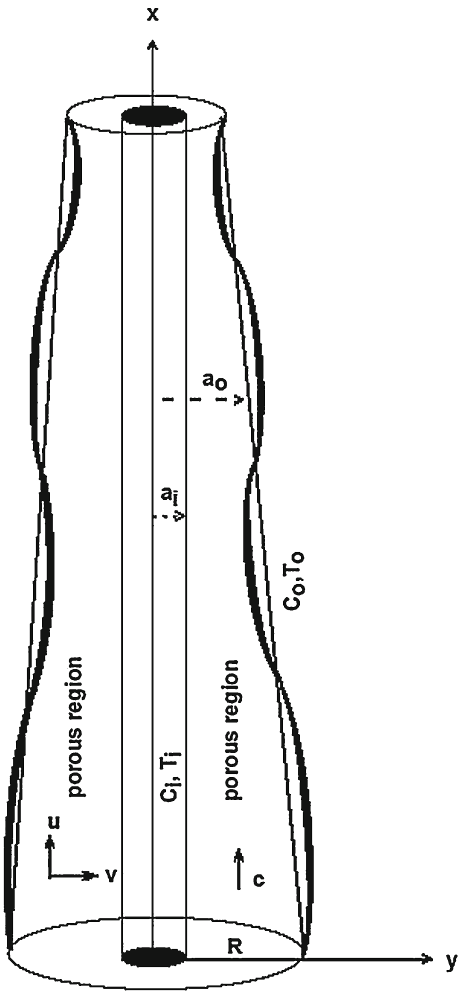

The mass transfer is the flow along the wall surface of the coaxial tubes (in the gap between them) that contains a species A slightly soluble in the fluid B. Let C_0 be the solubility of A in B, and concentration of A at the inner tube is $C_{\rm i}$. Also, let the reaction of a species A with B be the first-order homogeneous chemical reaction of rate constant k_1. The concentration of dissolved A is considered small enough. Under these assumptions, the governing momentum, continuity, temperature, and concentration equations for this problem can be written as

$$\rho\left(\frac{\partial\bar{u}}{\partial\bar{t}}+\bar{u}\frac{\partial\bar{u}}{\partial\bar{x}}+\bar{v}\frac{\partial\bar{u}}{\partial\bar{y}}\right)=-\frac{\partial\bar{p}}{\partial\bar{x}}+\frac{\partial\bar{S}_{\overline{xx}}}{\partial\bar{x}}+\frac{\partial\bar{S}_{\overline{xy}}}{\partial\bar{y}}+\rho g\beta\left(T-\overline{T}\right)+\rho g\beta^{*}\left(C-\overline{C}\right)-\frac{\mu}{k_0}\bar{u} \quad (3)$$

$$\rho\left(\frac{\partial\bar{v}}{\partial\bar{t}}+\bar{u}\frac{\partial\bar{v}}{\partial\bar{x}}+\bar{v}\frac{\partial\bar{v}}{\partial\bar{y}}\right)=-\frac{\partial\bar{p}}{\partial\bar{y}}+\frac{\partial\bar{S}_{\overline{xy}}}{\partial\bar{x}}+\frac{\partial\bar{S}_{\overline{yy}}}{\partial\bar{y}}-\frac{\mu}{k_0}\bar{v} \quad (4)$$

$$\frac{\partial\bar{u}}{\partial\bar{x}}+\frac{\partial\bar{v}}{\partial\bar{y}}=0 \quad (5)$$

$$\rho c_p\left(\frac{\partial T}{\partial \bar{t}}+\bar{u}\frac{\partial T}{\partial \bar{x}}+\bar{v}\frac{\partial T}{\partial \bar{y}}\right)=k\nabla^2 T+\frac{\mu}{k_0}\overline{q}(\bar{u}+\bar{v}) \tag{6}$$

$$\frac{\partial C}{\partial \bar{t}}+\bar{u}\frac{\partial C}{\partial \bar{x}}+\bar{v}\frac{\partial C}{\partial \bar{y}}=D\nabla^2 C-k_1 C \tag{7}$$

Here, $\overline{q}=\sqrt{\bar{u}^2+\bar{v}^2}$, $\bar{u}$ and $\bar{v}$ are the velocities in the $\bar{x}$, $\bar{y}$ directions, respectively, T is the temperature, C is the concentration, ρ is the fluid density, $\bar{p}$ is the pressure, μ is the dynamic viscosity, k_0 is the permeability of porous medium, g is the acceleration due to gravity, β is the volumetric expansion coefficient, β^* is the coefficient of expansion with concentration, $\bar{T}$ is the mean of $T_{\rm i}$ and $T_{\rm o}$, $\bar{C}$ is the mean of $C_{\rm i}$ and $C_{\rm o}$, k is the thermal conductivity, c_p is the specific heat at constant pressure, D is the mass diffusivity, and k_1 is the chemical reaction parameter.

The constitutive equations for an incompressible Jeffrey fluid are (Hayat et al. 2006, 2008)

$$\begin{aligned}\bar{\tau}&=-\bar{p}I+\bar{S}\\ \bar{S}&=\frac{\mu}{1+\lambda_1}\left(\dot{\gamma}+\lambda_2\ddot{\gamma}\right)\end{aligned} \tag{8}$$

where $\bar{\tau}$ and $\bar{S}$ are Cauchy stress tensor and extra stress tensor, respectively, I is the identity tensor, λ_1 is the relaxation time, λ_2 is the retardation time, $\dot{\gamma}$ is the shear rate, and dots over the quantities indicate differentiation with respect to time.

The boundary conditions for this system are given by

$$\begin{aligned}&\bar{u}=0,\quad \bar{v}=0\quad \text{at }\ \bar{y}=\bar{y}_1\\ &\bar{u}=0,\quad \bar{v}=\frac{\partial \bar{y}_2}{\partial \bar{t}}\quad \text{at }\bar{y}=\bar{y}_2\\ &T=T_{\rm i},\quad C=C_{\rm i}\quad \text{at }\bar{y}=\bar{y}_1\\ &T=T_{\rm o},\quad C=C_{\rm o}\quad \text{at }\bar{y}=\bar{y}_2\end{aligned} \tag{9}$$

It is convenient to non-dimensionalize the variables appearing in Eqs. 1–9 as follows

$$\begin{aligned}&x=\frac{\bar{x}}{\lambda},\quad y=\frac{\bar{y}}{R},\quad u=\frac{\bar{u}}{c},\quad v=\frac{\lambda\bar{v}}{Rc},\quad p=\frac{R^2}{\lambda\mu c}\bar{p},\quad t=\frac{\bar{t}c}{\lambda},\\ &Re=\frac{\rho cR}{\mu},\quad S=\frac{R\bar{S}}{\mu c},\quad \delta=\frac{R}{\lambda},\quad y_1=\frac{\bar{y}_1}{R}=\eta,\quad y_2=\frac{\bar{y}_2}{R},\\ &\phi=\frac{b}{R},\quad \Theta=\frac{T-\bar{T}}{T_{\rm i}-\bar{T}},\quad \Phi=\frac{C-\bar{C}}{C_{\rm i}-\bar{C}},\quad n=\frac{T_{\rm o}-\bar{T}}{T_{\rm i}-\bar{T}},\\ &m=\frac{C_{\rm o}-\bar{C}}{C_{\rm i}-\bar{C}},\quad \varepsilon^2=\frac{R^2}{k_0},\quad \nu=\frac{\mu}{\rho},\quad G_T=\frac{g\beta(T_{\rm i}-\bar{T})R^2}{\nu c},\\ &G_C=\frac{g\beta^*(C_{\rm i}-\bar{C})R^2}{\nu c},\quad Pr=\frac{\rho c_p\nu}{k},\quad E_C=\frac{\mu c^2}{k(T_{\rm i}-\bar{T})},\\ &Sr=\frac{\nu}{D},\quad \gamma=\frac{k_1R^2}{\nu}\end{aligned} \tag{10}$$

where Re is the Reynolds number, δ is the wave number, η is radius ratio, $\phi(<1)$ is the amplitude ratio, n is the wall-temperature ratio, m is the wall-concentration ratio, ε^2 is the porous parameter, G_T is the Grashof number, G_C is the modified Grashof number, ν is the kinematic viscosity, Pr is the Prandtl number, E_C is the Eckert number, Sr is the Soret number, and γ is the non-dimensional chemical reaction parameter.

In terms of these variables, Eqs. 3–7 become

$$\delta Re\left(\frac{\partial u}{\partial t}+u\frac{\partial u}{\partial x}+v\frac{\partial u}{\partial y}\right)=-\frac{\partial p}{\partial x}+\delta\frac{\partial S_{xx}}{\partial x}+\frac{\partial S_{xy}}{\partial y}-\varepsilon^2u+G_T\Theta +G_C\Phi \tag{11}$$

$$\delta^3 Re\left(\frac{\partial v}{\partial t}+u\frac{\partial v}{\partial x}+v\frac{\partial v}{\partial y}\right)=-\frac{\partial p}{\partial y}+\delta^2\frac{\partial S_{xy}}{\partial x}+\delta\frac{\partial S_{yy}}{\partial y}-\delta^2\varepsilon^2 v \tag{12}$$

$$\frac{\partial u}{\partial x}+\frac{\partial v}{\partial y}=0 \tag{13}$$

$$\delta Re\left(\frac{\partial \Theta}{\partial t}+u\frac{\partial \Theta}{\partial x}+v\frac{\partial \Theta}{\partial y}\right)=\frac{1}{Pr}\left\{\delta^2\frac{\partial^2\Theta}{\partial x^2}+\frac{\partial^2\Theta}{\partial y^2} +\varepsilon^2E_C(u+\delta v)\sqrt{u^2+\delta^2v^2}\right\} \tag{14}$$

$$\delta Re\left(\frac{\partial \Phi}{\partial t}+u\frac{\partial \Phi}{\partial x}+v\frac{\partial \Phi}{\partial y}\right)=\frac{1}{Sr}\left\{\delta^2\frac{\partial^2\Phi}{\partial x^2}+\frac{\partial^2\Phi}{\partial y^2}\right\}-\gamma\Phi \tag{15}$$

while Eq. 8 turns into its dimensionless form, reading

$$\begin{aligned} S_{xx}&=\frac{2\delta}{1+\lambda_1}\left[1+\frac{\lambda_2\delta c}{a_{20}}\left(\frac{\partial}{\partial t}+u\frac{\partial}{\partial x}+v\frac{\partial}{\partial y}\right)\right]\frac{\partial u}{\partial x},\\ S_{xy}&=\frac{1}{1+\lambda_1}\left[1+\frac{\lambda_2\delta c}{a_{20}}\left(\frac{\partial}{\partial t}+u\frac{\partial}{\partial x}+v\frac{\partial}{\partial y}\right)\right]\left(\frac{\partial u}{\partial y}+\delta^2\frac{\partial v}{\partial x}\right),\\ S_{yy}&=\frac{2\delta}{1+\lambda_1}\left[1+\frac{\lambda_2\delta c}{a_{20}}\left(\frac{\partial}{\partial t}+u\frac{\partial}{\partial x}+v\frac{\partial}{\partial y}\right)\right]\frac{\partial v}{\partial y}\end{aligned} \tag{16}$$

Thus, the boundary conditions (9) in their dimensionless form read

$$\begin{aligned} u&=0, \quad v=0 \quad \text{at } y=y_1\\ u&=0, \quad v=\frac{\partial y_2}{\partial t} \quad \text{at } y=y_2\\ \Theta&=n, \quad \Phi=m \quad \text{at } y=y_1\\ \Theta&=1, \quad \Phi=1 \quad \text{at } y=y_2\end{aligned} \tag{17}$$

where

$$y_2=1-\frac{\lambda}{R}x\tan\psi+\phi\sin[2\pi\,(x-t)]$$

Using the long-wavelength approximation to our analysis as described in Ref. Shapiro et al. (1969), then the field Eqs. 11, 12, and 14–16 now give

$$\frac{\partial p}{\partial x}=\frac{1}{1+\lambda_1}\frac{\partial^2 u}{\partial y^2}-\widetilde{\varepsilon}^2u+G_T\Theta+G_C\Phi \tag{18}$$

$$\frac{\partial p}{\partial y}=0 \tag{19}$$

$$\frac{\partial^2\Theta}{\partial y^2}=-\widetilde{\varepsilon}^2E_Cu^2 \tag{20}$$

$$\frac{\partial^2\Phi}{\partial y^2}=Sr\gamma\Phi \tag{21}$$

where $\widetilde{\varepsilon}^2 = \varepsilon^2/(1+\lambda_1)$. Equation 19 indicates that p is independent of y (i.e., $p \neq p(y)$). Hence, p is a function of x and t only.

3 Rate of Volume Flow

We have transformed the moving coordinates (x^*, y^*) which move with the same wave velocity, c, in the positive $\bar{x}$-direction, to stationary coordinate $(\bar{x}, \bar{y})$ as follows

$$\bar{x} = x^* + c\bar{t}, \quad \bar{u} = u^* + c, \quad \bar{v} = v^* \tag{22}$$

where u^*, v^* and $\bar{u}$, $\bar{v}$ are the velocity components in the corresponding coordinate systems. The instantaneous volume flow rate in the stationary coordinates is given by

$$Q(\overline{x}, \overline{t}) = \int_{\bar{y}_1}^{\bar{y}_2} \overline{u}(\overline{x}, \overline{y}, \overline{t})\mathrm{d}\overline{y} \tag{23}$$

where $\bar{y}_2$ is a function of $\overline{x}$, $\overline{t}$. The rate of volume flow in the moving coordinates through each section, q^*, is a constant, independent of both $\overline{x}$ and $\overline{t}$. It is calculated as

$$q^* = \int_{\bar{y}_1}^{\bar{y}_2} u^*(x^*, y^*)\mathrm{d}y^* \tag{24}$$

Using Eq. 22, one finds that the two rates of volume flow are related by

$$Q = q^* + c(\bar{y}_2 - \bar{y}_1) \tag{25}$$

The time-averaged flow over a period $\Upsilon = \lambda/c$ at a fixed position $\bar{x}$ is defined as

$$\overline{Q} = \frac{1}{\Upsilon} \int_0^{\Upsilon} Q\mathrm{d}\bar{t} \tag{26}$$

Invoking Eq. 25 into Eq. 26 and then integrating one can write

$$\overline{Q} = q^* + c(a_2 - a_1) \tag{27}$$

Substituting from Eq. 27 into Eq. 25, we obtain

$$Q = \overline{Q} + cb\sin\left[\frac{2\pi}{\lambda}\left(\overline{x} - c\overline{t}\right)\right] \tag{28}$$

Defining the dimensionless mean flows f and F as

$$f = \frac{Q}{cR} \quad \text{and} \quad F = \frac{\overline{Q}}{cR} \tag{29}$$

Eq. 28 can be written as

$$f = F + \phi\sin\left[2\pi(x - t)\right] \tag{30}$$

where

$$f = \int_{y_1}^{y_2} u\mathrm{d}y \tag{31}$$

4 Method of Solution

Because, it is not possible to get closed form solutions for Eqs. 18, 20, and 21 for arbitrary values of all the parameters, we seek the solution of the problem as a power series expansion in the small parameter $\widetilde{\varepsilon}^2$, see Refs. Srinivas and Gayathri (2009), Srinivas and Kothandapani (2009), as follows

$$\begin{aligned} u &= u_0 + \widetilde{\varepsilon}^2 u_1 + O(\widetilde{\varepsilon}^4) \\ p &= p_0 + \widetilde{\varepsilon}^2 p_1 + O(\widetilde{\varepsilon}^4) \\ \Theta &= \Theta_0 + \widetilde{\varepsilon}^2 \Theta_1 + O(\widetilde{\varepsilon}^4) \\ \Phi &= \Phi_0 + \widetilde{\varepsilon}^2 \Phi_1 + O(\widetilde{\varepsilon}^4) \end{aligned} \tag{32}$$

Substituting Eq. 32 in Eqs. 18, 20, and 21 and boundary conditions (17) and collecting equations coefficients of like powers of $\widetilde{\varepsilon}^2$, we get the following set of equations
Coefficient of $\widetilde{\varepsilon}^0$

$$\frac{\partial p_0}{\partial x} = \frac{1}{1+\lambda_1}\frac{\partial^2 u_0}{\partial y^2} + G_T\Theta_0 + G_C\Phi_0 \tag{33}$$

$$\frac{\partial^2 \Theta_0}{\partial y^2} = 0 \tag{34}$$

$$\frac{\partial^2 \Phi_0}{\partial y^2} = Sr\gamma\Phi_0 \tag{35}$$

and

$$\begin{aligned} &u_0 = 0, \quad \text{at} \quad y = y_1, \quad y = y_2 \\ &\Theta_0 = n, \quad \Phi_0 = m \quad \text{at} \quad y = y_1 \\ &\Theta_0 = 1, \quad \Phi_0 = 1 \quad \text{at} \quad y = y_2 \end{aligned} \tag{36}$$

Coefficient of $\widetilde{\varepsilon}^2$

$$\frac{\partial p_1}{\partial x} = \frac{1}{1+\lambda_1}\frac{\partial^2 u_1}{\partial y^2} - u_0 + G_T\Theta_1 + G_C\Phi_1 \tag{37}$$

$$\frac{\partial^2 \Theta_1}{\partial y^2} = -E_C u_0^2 \tag{38}$$

$$\frac{\partial^2 \Phi_1}{\partial y^2} = Sr\gamma\Phi_1 \tag{39}$$

and

$$u_1 = 0, \quad \text{at } y = \eta, \quad y = y_2 \tag{40}$$

$$\Theta_1 = 0, \quad \Phi_1 = 0 \quad \text{at } y = y_1, \ y = y_2 \tag{41}$$

Solving Eqs. 33–35 using (36) yield

$$u_0 = \frac{\partial p_0}{\partial x} a_1 + a_2 \tag{42}$$

$$\Theta_0 = c_1 y + c_2 \tag{43}$$

$$\Phi_0 = c_3 \exp(ay) + c_4 \exp(-ay) \tag{44}$$

where

$$
\begin{aligned}
a_1 &= \frac{1+\lambda_1}{2}\left(y^2 - \alpha_1 y + \alpha_2\right) \\
a_2 &= -\frac{1}{6}y\left(b_5 y^2 + 3b_6 y - 6b_3\right) - \alpha_3 \Phi_0 + b_4
\end{aligned}
\tag{45}
$$

in which all b's constants are given in the Appendix, and

$$
\begin{aligned}
\alpha_1 &= y_2 + y_1, \quad \alpha_2 = y_1 y_2, \quad \alpha_3 = \frac{(1+\lambda_1)G_C}{a^2}, \quad a^2 = Sr\gamma \\
c_1 &= \frac{(n-1)}{(y_1 - y_2)}, \quad c_2 = \frac{(y_1 - n y_2)}{(y_1 - y_2)} \\
c_3 &= \frac{\left[m \exp(-a y_2) - \exp(-a y_1)\right]}{2\sinh\left[a(y_1 - y_2)\right]} \\
c_4 &= \frac{\left[\exp(a y_1) - m \exp(a y_2)\right]}{2\sinh\left[a\,(y_1 - y_2)\right]}
\end{aligned}
$$

The volume flow rate f_0 in the stationary coordinates is given by

$$
f_0 = \int_{y_1}^{y_2} u_0 \mathrm{d}y \tag{46}
$$

Substituting from Eq. 42 in Eq. 46 and solving the resulting equation for $\partial p_0/\partial x$, yields

$$
\frac{\partial p_0}{\partial x} = \frac{2}{(1+\lambda_1)\xi}\left[f_0 + a_3\right] \tag{47}
$$

where

$$
\begin{aligned}
\xi &= \frac{1}{3}\left(y_2^3 - y_1^3\right) - \frac{\alpha_1}{2}\left(y_2^2 - y_1^2\right) + \alpha_2\left(y_2 - y_1\right) \\
a_3 &= \frac{1}{6}\left[\frac{b_5}{4}\left(y_2^4 - y_1^4\right) + b_6\left(y_2^3 - y_1^3\right) - 3b_3\left(y_2^2 - y_1^2\right)\right] + \frac{\alpha_3}{a^2}\left(\frac{\Phi_0^{(2)}}{\partial y} - \frac{\Phi_0^{(1)}}{\partial y}\right) \\
&\quad - b_4(y_2 - y_1)
\end{aligned}
\tag{48}
$$

Substituting from Eq. 42 into Eq. 38, and solving the resulting equation subjected to the boundary conditions (41), we find that

$$
\Theta_1 = \left(\frac{\partial p_0}{\partial x}\right)^2 a_4 + \frac{\partial p_0}{\partial x} a_5 + a_6 \tag{49}
$$

where

$$a_4 = \frac{E_C(1+\lambda_1)^2}{8}\left\{-\frac{2}{30}y^6 + \frac{\alpha_1}{5}y^5 - b_{14}y^4 + \frac{2\alpha_1\alpha_2}{3}y^3 - \alpha_2^2 y^2 + b_{29}y + b_{30}\right\}$$

$$a_5 = (1+\lambda_1)E_C\left\{\frac{b_5}{252}y^7 + b_{15}y^6 - b_{16}y^5 + b_{17}y^4 + b_{18}y^3 - \frac{\alpha_2 b_4}{2}y^2 + b_{31}y + b_{32} + \left[b_{19} - \frac{\alpha_3}{a^2}\left(\alpha_1 y - y^2\right)\right]\Phi_0 + b_{20}\frac{\partial \Phi_0}{\partial y}\right\} \tag{50}$$

$$a_6 = E_C\left\{-\frac{b_5^2}{2016}y^8 - \frac{b_5 b_6}{252}y^7 + b_7 y^6 + b_8 y^5 + b_9 y^4 - \frac{b_3 b_4}{3}y^3 - b_{13}y^2 + b_{27}y + b_{28} + \left[b_{10} + \frac{2\alpha_3}{a^4}\left(2b_6 y + b_5 y^2\right)\right]\frac{\partial \Phi_0}{\partial y} + \left[b_{11} + b_{12}y - \frac{\alpha_3}{a^2}\left(b_6 y^2 + \frac{b_5}{3}y^3\right)\right]\Phi_0 - \left(\frac{\alpha_3}{2a}\Phi_0\right)^2\right\}$$

Solving Eq. 39 subject to the boundary conditions (41), we obtain

$$\Phi_1 = 0 \tag{51}$$

We determine the first-order velocity u_1 by substituting Eqs. 42, 49, and 51 into Eq. 37 subject to the boundary conditions (40), we find that

$$u_1 = \frac{\partial p_1}{\partial x}a_1 + \left(\frac{\partial p_0}{\partial x}\right)^2 a_7 + \frac{\partial p_0}{\partial x}a_8 + a_9 \tag{52}$$

where

$$a_7 = \frac{(1+\lambda_1)^3}{16}E_C G_T\left\{\frac{1}{420}y^8 - \frac{\alpha_1}{105}y^7 + \frac{b_{15}}{15}y^6 - \frac{\alpha_1\alpha_2}{15}y^5 + \frac{\alpha_2^2}{6}y^4 - \frac{b_{29}}{3}y^3 - b_{30}y^2 + b_{51}y + b_{52}\right\}$$

$$a_8 = (1+\lambda_1)^2 E_C G_T\left\{-\frac{b_5}{18144}y^9 - \frac{b_{15}}{56}y^8 + \frac{b_{16}}{42}y^7 - \frac{b_{17}}{30}y^6 - \frac{b_{18}}{20}y^5 + b_{40}y^4 - b_{41}y^3 - b_{42}y^2 + b_{53}y + b_{54} - \left(b_{43} - \frac{\alpha_1\alpha_3}{a^4}y + \frac{\alpha_3}{a^4}y^2\right)\Phi_0 - \left(b_{44} - \frac{4\alpha_3}{a^6}y\right)\frac{\partial \Phi_0}{\partial y}\right\} \tag{53}$$

$$a_9 = (1+\lambda_1)E_C G_T\left\{\frac{b_5^2}{181440}y^{10} + \frac{b_5 b_6}{18144}y^9 - \frac{b_7}{56}y^8 - \frac{b_8}{42}y^7 - \frac{b_9}{30}y^6 + b_{33}y^5 + b_{34}y^4 + b_{35}y^3 + b_{36}y^2 + b_{55}y + b_{56} + \left(b_{37} + b_{38}y + \frac{\alpha_3 b_6}{a^4}y^2 + \frac{\alpha_3 b_5}{3a^4}y^3\right)\Phi_0\right.$$

$$+\left(b_{39}-\frac{8\alpha_3 b_6}{a^6}y-\frac{4\alpha_3 b_5}{a^6}y^2\right)\frac{\partial\Phi_0}{\partial y}+\left(\frac{\alpha_3}{4a^2}\Phi_0\right)^2\Bigg\}$$

The volume flow rate f_1 in the stationary coordinates is given by

$$f_1=\int_{y_1}^{y_2}u_1\mathrm{d}y \tag{54}$$

substituting from Eq. 51 in Eq. 53 and solving the resulting equation for $\partial p_1/\partial x$ give

$$\frac{\partial p_1}{\partial x}=\frac{2}{(1+\lambda_1)\xi}\left[f_1-\left(\frac{\partial p_0}{\partial x}\right)^2 a_{10}-\frac{\partial p_0}{\partial x}a_{11}-a_{12}\right] \tag{55}$$

where

$$a_{10}=E_C G_T\frac{(1+\lambda_1)^3}{16}\left\{\frac{1}{3780}\left(y_2^9-y_1^9\right)-\frac{\alpha_1}{840}\left(y_2^8-y_1^8\right)+\frac{b_{15}}{105}\left(y_2^7-y_1^7\right)\right.$$
$$-\frac{\alpha_1\alpha_2}{90}\left(y_2^6-y_1^6\right)+\frac{\alpha_2^2}{30}\left(y_2^5-y_1^5\right)-\frac{b_{29}}{12}\left(y_2^4-y_1^4\right)-\frac{b_{30}}{3}\left(y_2^3-y_1^3\right)$$
$$\left.+\frac{b_{51}}{2}\left(y_2^2-y_1^2\right)+b_{52}\left(y_2-y_1\right)\right\}$$
$$a_{11}=E_C G_T(1+\lambda_1)^2\left\{-\frac{b_5}{181440}\left(y_2^{10}-y_1^{10}\right)+\frac{b_{15}}{504}\left(y_2^9-y_1^9\right)\right.$$
$$+\frac{b_{16}}{336}\left(y_2^8-y_1^8\right)-\frac{b_{17}}{210}\left(y_2^7-y_1^7\right)-\frac{b_{18}}{120}\left(y_2^6-y_1^6\right)+\frac{b_{40}}{5}\left(y_2^5-y_1^5\right)$$
$$-\frac{b_{41}}{4}\left(y_2^4-y_1^4\right)-\frac{b_{42}}{3}\left(y_2^3-y_1^3\right)+\frac{b_{53}}{2}\left(y_2^2-y_1^2\right)+b_{54}\left(y_2-y_1\right)$$
$$-b_{57}\left(\Phi_0^{(2)}-\Phi_0^{(1)}\right)+\frac{6\alpha_3}{a^6}\left(y_2\Phi_0^{(2)}-y_1\Phi_0^{(1)}\right)-b_{58}\left(\frac{\partial\Phi_0^{(2)}}{\partial y}-\frac{\partial\Phi_0^{(1)}}{\partial y}\right)$$
$$\left.+\frac{\alpha_3}{a^8}\left[y_2\left(\alpha_1-y_2\right)\frac{\partial\Phi_0^{(2)}}{\partial y}-y_1\left(\alpha_1-y_1\right)\frac{\partial\Phi_0^{(1)}}{\partial y}\right]\right\}$$
$$a_{12}=E_C G_T(1+\lambda_1)\left\{\frac{b_5^2}{1995840}\left(y_2^{11}-y_1^{11}\right)+\frac{b_5 b_6}{181440}\left(y_2^{10}-y_1^{10}\right)\right.$$
$$-\frac{b_7}{504}\left(y_2^9-y_1^9\right)-\frac{b_8}{336}\left(y_2^8-y_1^8\right)-\frac{b_9}{210}\left(y_2^7-y_1^7\right)+\frac{b_{33}}{6}\left(y_2^6-y_1^6\right)$$
$$+\frac{b_{34}}{5}\left(y_2^5-y_1^5\right)+\frac{b_{35}}{4}\left(y_2^4-y_1^4\right)+\frac{b_{36}}{3}\left(y_2^3-y_1^3\right)+\frac{b_{55}}{2}\left(y_2^2-y_1^2\right)$$
$$+b_{59}\left(y_2-y_1\right)+b_{60}\left(\Phi_0^{(2)}-\Phi_0^{(1)}\right)-\frac{5\alpha_3}{a^6}[y_2\left(2b_5+b_6 y_2\right)\Phi_0^{(2)}$$
$$-y_1\left(2b_5+b_6 y_1\right)\Phi_0^{(1)}]+b_{61}\left(\frac{\partial\Phi_0^{(2)}}{\partial y}-\frac{\partial\Phi_0^{(1)}}{\partial y}\right)+b_{62}\left(y_2\frac{\partial\Phi_0^{(2)}}{\partial y}\right.$$
$$\left.-y_1\frac{\partial\Phi_0^{(1)}}{\partial y}\right)+\frac{\alpha_3}{a^6}\left[y_2^2\left(b_6+\frac{b_5}{3}y_2\right)\frac{\partial\Phi_0^{(2)}}{\partial y}-y_1^2\left(b_6+\frac{b_5}{3}y_1\right)\frac{\partial\Phi_0^{(1)}}{\partial y}\right]$$

$$+\frac{\alpha_3^2}{32a^7}\left(\Phi_0^{(2)}\frac{\partial\Phi_0^{(2)}}{\partial y}-\Phi_0^{(1)}\frac{\partial\Phi_0^{(1)}}{\partial y}\right) \tag{56}$$

The constants b_{i} ($i = 1, ..., 62$) are defined in the Appendix.

Substituting from Eqs. 47 and 55 into Eq. 32, then the expression for the pressure gradient takes the following form

$$\frac{\partial p}{\partial x}=\frac{2}{(1+\lambda_1)\xi}\left\{(f_0+a_3)+\tilde{\varepsilon}^2\left[f_1-\left(\frac{2}{(1+\lambda_1)\xi}\right)^2(f_0+2a_3)\,f_0a_{10}\right.\right.$$
$$\left.\left.-\frac{2}{(1+\lambda_1)\xi}a_{11}f_0-\left(\frac{2a_3}{(1+\lambda_1)\xi}\right)^2a_{10}-\frac{2a_3a_{11}}{(1+\lambda_1)\xi}-a_{12}\right]\right\} \tag{57}$$

The results of our analysis can be expressed to second order by defining

$$f=f_0+\tilde{\varepsilon}^2f_1 \tag{58}$$

then substituting $f_0 = f - \tilde{\varepsilon}^2 f_1$ in Eq. 57 and neglecting the terms greater than $O(\tilde{\varepsilon}^2)$, we find

$$\frac{\partial p}{\partial x}=\frac{2}{(1+\lambda_1)\xi}\left\{(f+a_3)-\tilde{\varepsilon}^2\left[\left(\frac{2}{(1+\lambda_1)\xi}\right)^2(f+2a_3)\,fa_{10}\right.\right.$$
$$\left.\left.+\frac{2}{(1+\lambda_1)\xi}a_{11}f+\left(\frac{2a_3}{(1+\lambda_1)\xi}\right)^2a_{10}+\frac{2a_3a_{11}}{(1+\lambda_1)\xi}+a_{12}\right]\right\} \tag{59}$$

The non-dimensional expressions for pressure rise per wavelength $\Delta P_\lambda(t)$ and frictional forces on the inner $F_\lambda^{(\mathrm{i})}(t)$ and outer $F_\lambda^{(\mathrm{o})}(t)$ tubes are directly given by Misra and Pandey (1995), Elshehawey et al. (1998), Mekheimer (2004), Elshehawey et al. (2005), and Mekheimer (2005)

$$\Delta P_\lambda(t)=\int_0^1\left(\frac{\partial p}{\partial x}\right)\mathrm{d}x \tag{60}$$

$$F_\lambda^{(i)}(t)=\int_0^1 y_1^2\left(-\frac{\partial p}{\partial x}\right)\mathrm{d}x \tag{61}$$

$$F_\lambda^{(o)}(t)=\int_0^1 y_2^2\left(-\frac{\partial p}{\partial x}\right)\mathrm{d}x \tag{62}$$

Substituting from Eq. 59 into Eqs. 60–62 and then evaluating the integrations numerically for several values of the parameters included, using the Software Fortran 90 Ellis et al. (1994), and the obtained results are discussed in Sect. 6.

Note that if the tube length is finite but equals an integral number of wavelengths, and if the pressure difference between the ends of the tube is constant, the flow is steady in the wave frame. Hence, when we computed the pressure drop $\Delta P_L(t)$, we used the inlet and outlet flows boundary conditions $p = p_0$ at $x = 0$, and $p = p_L$ at $x = L$. Then, the pressure drop $\Delta P_L(t)$ in the tube length L in the non-dimensional form is obtained as $\Delta P_\lambda(t) = \int_0^{\Lambda}\left(\frac{\partial p}{\partial x}\right)\mathrm{d}x$, where $\Lambda = L/\lambda$, and we have taken $L = \lambda = 8.01$ cm.

5 Characteristic Coefficients

The expression for the axial velocity component u, temperature Θ, and concentration Φ, respectively can be obtained from Eqs. 32, 42–44, 49, 51, and 52, and they take the following forms

$$u = a_2 + \frac{\partial p}{\partial x} a_1 + \widetilde{\varepsilon}^2 \left[a_9 + \left(\frac{2a_3}{(1+\lambda_1)\xi} \right)^2 a_7 + \frac{2a_3 a_8}{(1+\lambda_1)\xi} \right] + \frac{2\widetilde{\varepsilon}^2 f_0}{(1+\lambda_1)\xi} \left[\frac{2}{(1+\lambda_1)\xi} (f_0 + 2a_3) a_7 + a_8 \right] \tag{63}$$

$$\Theta = c_1 y + c_2 + \widetilde{\varepsilon}^2 \left\{ \left(\frac{2}{(1+\lambda_1)\xi} \right)^2 \left(f_0^2 + 2a_3 f_0 + a_3^2 \right) a_4 + \frac{2a_5 f_0}{(1+\lambda_1)\xi} + \frac{2a_3 a_5}{(1+\lambda_1)\xi} + a_6 \right\} \tag{64}$$

$$\Phi = c_3 \exp(ay) + c_4(-ay) \tag{65}$$

Substituting from Eq. 58 in Eqs. 63 and 64 and neglecting the terms greater than $O(\widetilde{\varepsilon}^2)$, we get

$$u = a_2 + \frac{\partial p}{\partial x} a_1 + \widetilde{\varepsilon}^2 \left[a_9 + \left(\frac{2a_3}{(1+\lambda_1)\xi} \right)^2 a_7 + \frac{2a_3 a_8}{(1+\lambda_1)\xi} \right] + \frac{2\varepsilon^2 f}{(1+\lambda_1)\xi} \left[\frac{2}{(1+\lambda_1)\xi} (f + 2a_3) a_7 + a_8 \right] \tag{66}$$

$$\Theta = c_1 y + c_2 + \widetilde{\varepsilon}^2 \left\{ \left(\frac{2}{(1+\lambda_1)\xi} \right)^2 \left(f^2 + 2a_3 f + a_3^2 \right) a_4 + \frac{2a_5 f}{(1+\lambda_1)\xi} + \frac{2a_3 a_5}{(1+\lambda_1)\xi} + a_6 \right\} \tag{67}$$

Now, the skin friction coefficient τ, the heat transfer coefficient (Nusselt number) Nu, and the mass transfer coefficient (Sherwood number) Sh at the wall of both inner and outer tubes are defined respectively by Massey (1989)

$$\tau = \frac{1}{1+\lambda_1} \left(\frac{\partial u}{\partial y} \right)_w, \quad Nu = \left(\frac{\partial \Theta}{\partial y} \right)_w, \quad Sh = \left(\frac{\partial \Phi}{\partial y} \right)_w \quad \text{at } w = y_1,\ y_2 \tag{68}$$

The expressions for τ, Nu, and Sh have been obtained by substituting from Eqs. 65–67 into Eq. 68 respectively, and then they have been evaluated numerically for several values of the parameters of the problem, using the Software Fortran 90 (Ellis et al. 1994). The obtained results will be discussed in the next section.

6 Results and Discussion

It is clear that we have to choose the porosity parameter less than one because we have used the perturbation method with the porosity parameter. Moreover, the approximation we have used (long-wavelength approximation) restricted us in choosing the values of propagation velocity, wavelength, and radius of the tube such that the wave number is neglected and Reynolds

Fig. 2 The variation of $\Delta P_\lambda(t)$ versus F with fixed $\psi = 0.5,\ \eta = 0.32,$ $Sr = 0.6,\ E_C = 3,\ \gamma = 3,$ $\lambda_1 = 0.6,\ \phi = 0.1,$ $\widetilde{\varepsilon} = 0.3,\ G_C = 1,$ $n = 1.2,\ m = 1$, and $t = 0.3$ for different values of G_T

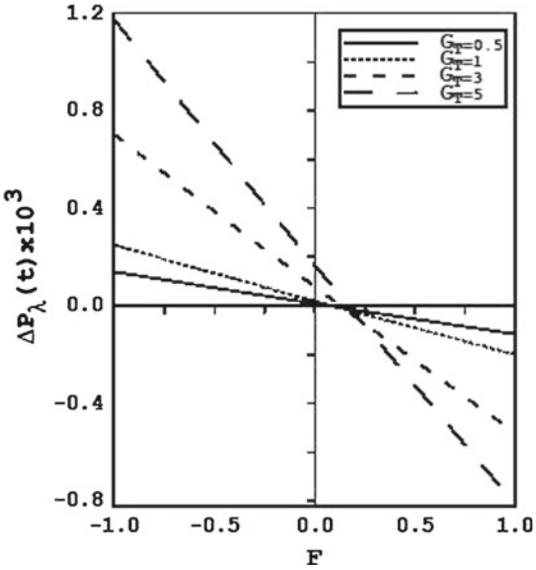

number is very small. As reported by Shukla et al. (1980) and Srivastava (1986), we use the following values of the human small intestine parameters as $R = 1.25$ cm, $c = 2$ cm/min, and $\lambda = 8.01$ cm. Furthermore, since most routine upper gastrointestinal endoscopes are from 8 to 11 mm in diameter as reported in Cotton and Williams (1990) and the radius of the small intestine is 1.25 cm as reported in Refs. Shukla et al. (1980), Srivastava (1986) then the radius ratio η takes the values $0.32,\ 0.38$, and 0.44, and since $\eta = a_i/R$, $R = 1.25$ cm, then the radius of the inner tube takes one of the values $a_i = 0.4,\ 0.475,$ *and* 0.55 cm. It should be noted also here that we have chosen the parameter $\varepsilon^2 = 0.01,\ 0.05,\ 0.1,\ 0.5,\ 1,\ 2,$ and 3 (see Ref. Hayat et al. 2008). Moreover, the values of permeability parameter can be obtained using the relation $\varepsilon^2 = R^2/k_0$, where R is a constant.

Here, our aim interest is to study the effects of various emerging parameters such as $\psi,\ \phi,\ \lambda_1,\ \widetilde{\varepsilon},\ Sr,\ \gamma,\ E_C,\ G_T,\ G_C$, and η on the pressure rise $\Delta P_\lambda(t)$, the inner friction force $F_\lambda^{(\mathrm{i})}(t)$ (on the inner surface) and the outer friction force $F_\lambda^{(\mathrm{o})}(t)$ (on the outer surface) over the tube length as a function of flow rate F. The skin friction coefficient τ, the heat transfer coefficient (Nusselt number) Nu, and the mass transfer coefficient (Sherwood number) Sh at the wall of both inner and outer tubes are evaluated numerically for different values of $\psi,\ \phi,\ \lambda_1,\ \widetilde{\varepsilon},\ Sr,\ \gamma,\ E_C,\ G_T,\ G_C,\ \eta$ and results are displayed graphically. Figures 2, 3, and 4 give the effects of some parameters ($G_T,\ \lambda_1,$ *and* γ) on $\Delta P_\lambda(t)$, and the effects of the other parameters are found to be similar to them; their figures are excluded here to avoid any kind of repetition. In these Figs. 2, 3, and 4, the regions $\Delta P_\lambda(t) > 0,\ \ F < 0$, and $\Delta P_\lambda(t) > 0,\ \ F > 0$; and $\Delta P_\lambda(t) < 0,\ \ F > 0$ are called retrograde pumping, peristaltic pumping, and augmented pumping, respectively.

In Fig. 2, the pressure rise $\Delta P_\lambda(t)$ is plotted against the flow rate F for various values of the Grashof number G_T, we observed that in the pumping region $\Delta P_\lambda(t) > 0$, an increase of G_T increases the pumping rate $\Delta P_\lambda(t)$, and in the copumping region $\Delta P_\lambda(t) < 0$, the pumping rate decreases by increasing G_T. Figure 2 shows also that there is an inversely linear relation between F and $\Delta P_\lambda(t)$, (i.e., for any G_T value, an increase in the flow rate F will decrease the pressure rise $\Delta P_\lambda(t)$, and vise versa) and that the maximum pressure

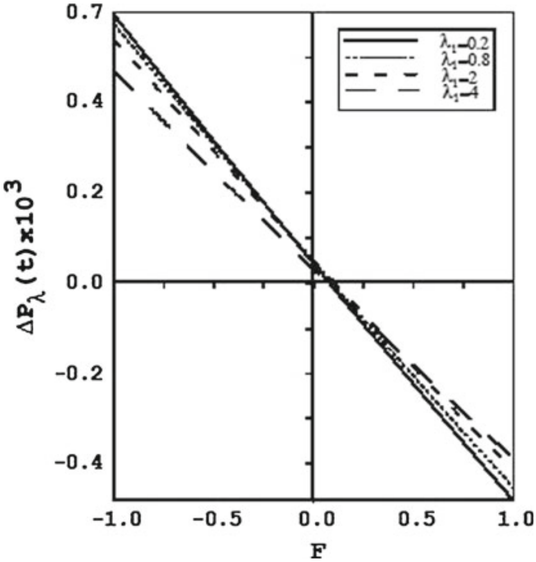

Fig. 3 The variation of $\Delta P_{\lambda}(t)$ versus F with fixed $\psi = 0.5,\ \eta = 0.32,\ Sr = 0.6,\ E_C = 3,\ \gamma = 3,\ \phi = 0.1,\ \widetilde{\varepsilon} = 0.5,\ G_C = 1,\ G_T = 1,\ n = 1.2,\ m = 1$, and $t = 0.3$ for different values of λ_1

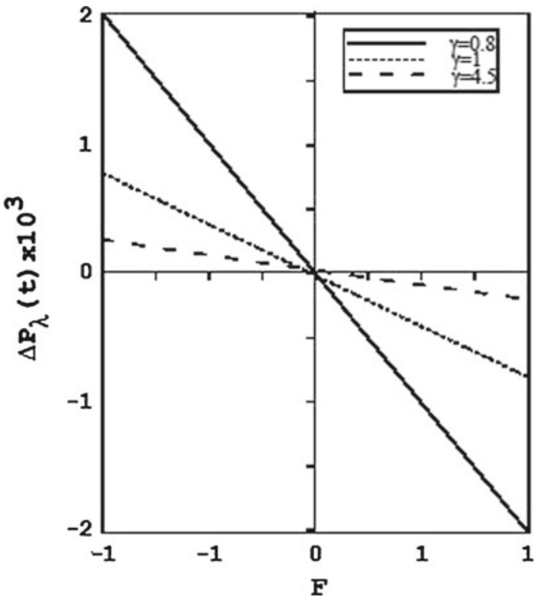

Fig. 4 The variation of $\Delta P_{\lambda}(t)$ versus F with fixed $\psi = 0.5,\ \eta = 0.32,\ Sr = 0.6,\ E_C = 3,\ \lambda_1 = 0.6,\ \phi = 0.1,\ \widetilde{\varepsilon} = 0.3,\ G_C = 1,\ G_T = 1,\ n = 1.2,\ m = 1$, and $t = 0.3$ for different values of γ

rise occurs at a negative value of the flow rate. Note that the peristaltic pumping region becomes slightly wider as G_T increases. The effects of the parameters $\psi,\ \phi,\ \eta,\ E_C$, and $\widetilde{\varepsilon}$ on $\Delta P_{\lambda}(t)$ and F are found to be similar to the effect of G_T on $\Delta P_{\lambda}(t)$ and F shown in Fig. 2. Figure 3 shows the variation of $\Delta P_{\lambda}(t)$ with F for different values of the ratio of relaxation to retardation time λ_1 on $\Delta P_{\lambda}(t)$ is a reverse to the effect of G_T on $\Delta P_{\lambda}(t)$, i.e., in the region $-1 \leqslant F < 0,\ \Delta P_{\lambda}(t)$ decreases by increasing λ_1, while in the region $0 \leqslant F \leqslant 1,\ \Delta P_{\lambda}(t)$ increases by increasing λ_1. Note that when $\lambda_1 < 4$, the peristaltic pumping region becomes slightly wider as λ_1 increases, and if $\lambda_1 \geqslant 4$, it is slightly narrow

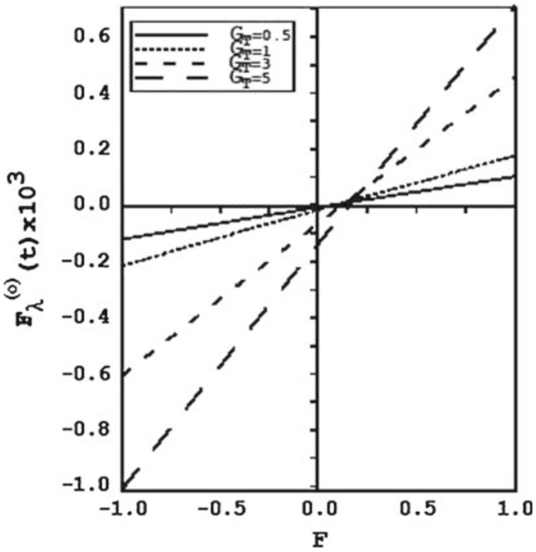

Fig. 5 The variation of $F_\lambda^{(o)}(t)$ versus F with fixed $\psi = 0.5,\ \eta = 0.32,\ Sr = 0.6,\ E_C = 3,\ \gamma = 3,\ \lambda_1 = 0.6,\ \phi = 0.1,\ \widetilde{\varepsilon} = 0.3,\ G_C = 1,\ n = 1.2,\ m = 1$, and $t = 0.3$ for different values of G_T

as λ_1 increases. Similar result can be found for the effect of G_C on $\Delta P_\lambda(t)$ and F, but in this case the peristaltic pumping region, for any λ_1 value, becomes slightly wider as λ_1 increases. Figure 4 shows the variation of $\Delta P_\lambda(t)$ with F for various values of the non-dimensional chemical reaction parameter γ. From this figure, we observe that the effect of γ on $\Delta P_\lambda(t)$ is similar to the effect of λ_1 on $\Delta P_\lambda(t)$ illustrated in Fig. 3, with the only difference that the peristaltic pumping region will disappear in this case, and all the obtained curves will intersect at the origin where $F = 0,\ \ \Delta P_\lambda(t) = 0$. The effect of the Soret number Sr on $\Delta P_\lambda(t)$ is found to be exactly similar the effect of γ on $\Delta P_\lambda(t)$ given by Fig. 4.

The outer and inner friction forces $F_\lambda^{(\mathrm{o})}(t)$ and $F_\lambda^{(\mathrm{i})}(t)$ appear at the outer and inner surfaces of the tubes, respectively, are plotted in Figs. 5 and 6 versus the flow rate F for various values of Grashof number G_T. We notice from these figures that, for any value of G_T, the outer friction $F_\lambda^{(\mathrm{o})}(t)$ has a greater value (positive or negative) than the inner friction $F_\lambda^{(\mathrm{i})}(t)$. Moreover, their behaviors being similar for the same value of G_T. We observe also that the effect of G_T on any of $F_\lambda^{(o)}(t)$ or $F_\lambda^{(i)}(t)$ can be considered as the same effect of G_T on pressure rise $\Delta P_\lambda(t)$ given by Fig. 2 but with a reflection about the horizontal axis F passing through the origin (0, 0). The above obtained results can be generalized for the effects of other parameters such as $\psi,\ \phi,\ \lambda_1,\ \widetilde{\varepsilon},\ Sr,\ \gamma,\ E_C,\ G_C$, and η on $F_\lambda^{(\mathrm{o})}(t)$ and $F_\lambda^{(\mathrm{i})}(t)$ in comparison with their effects on $\Delta P_\lambda(t)$.

Figures 7 and 8 show the behaviors of the skin friction τ at the inner and outer tubes with the flow rate F for different values of the modified Grashof number G_C and the radius ratio η, respectively. We observe from these figures that the skin friction τ at both tubes is a linear function of the flow rate F, and that the obtained curves will meet at $\tau = 0$. Figure 7 shows that the skin friction τ decreases (and increases) by increasing G_C when $\tau \gtrless 0$, respectively, while for any value of G_C, the skin friction τ increases (and decreases) by increasing the flow rate F at the inner or outer tubes, respectively. Also Fig. 8 shows that the skin friction τ increases (and decreases) by increasing η when $\tau \gtrless 0$, respectively, while for any value of η, the skin friction τ will have the same behavior by increasing the flow rate F as obtained in Fig. 7. The effects of the parameters $Sr,\ \ \gamma$, and λ_1 on the skin friction τ (figures are excluded) are found to be similar to the previous effect of G_C on τ given in Fig. 7, while

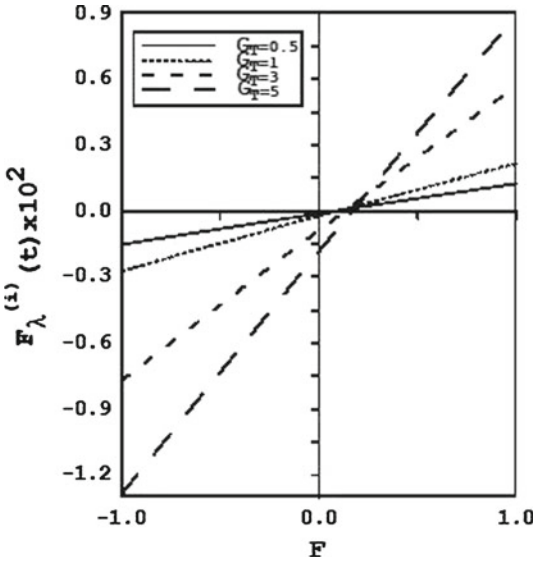

Fig. 6 The variation of $F_\lambda^{(i)}(t)$ versus F with fixed $\psi = 0.5,\ \eta = 0.32,\ Sr = 0.6,\ E_C = 3,\ \gamma = 3,\ \lambda_1 = 0.6,\ \phi = 0.1,\ \widetilde{\varepsilon} = 0.3,\ G_C = 1,\ n = 1.2,\ m = 1$, and $t = 0.3$ for different values of G_T

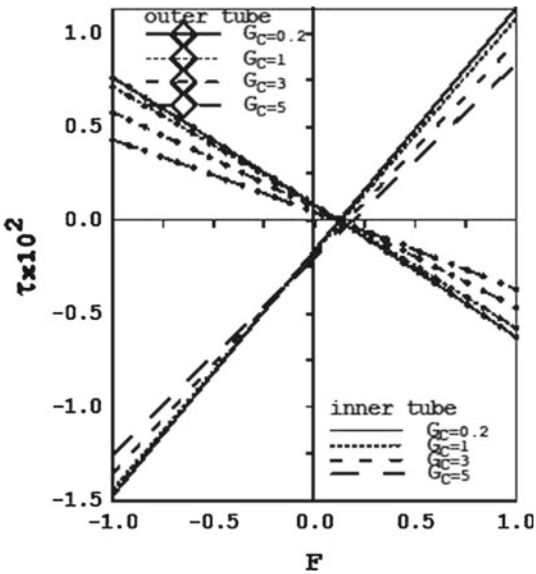

Fig. 7 The variation of τ versus F with fixed $\psi = 0.5,\ \eta = 0.32,\ Sr = 0.6,\ E_C = 3,\ \gamma = 3,\ \lambda_1 = 0.6,\ \phi = 0.1,\ \widetilde{\varepsilon} = 0.3,\ G_T = 1,\ n = 1.2,\ m = 1$, and $t = 0.3$ for different values of G_C

the effect of other parameters as $E_C,\ G_T,\ \widetilde{\varepsilon},\ \psi$, and ϕ on τ are found to be similar to the foregoing effect of η on τ given in Fig. 8, at the inner and outer tubes, respectively.

Figures 9 and 10 illustrate the behaviors of the Nusselt number Nu at the inner and outer tubes with the flow rate F for various values of the Grashof number G_T and the amplitude ratio ϕ, respectively. We notice from Fig. 9 that the resulting curves in this case will be similar to those obtained in Fig. 7 for the effect of G_C on τ except that they are parallel if we increase the value of G_T, and also that they will intersect at different points of negative Nu values which increase by increasing each of G_T and F. Also, Fig. 10 shows that the effect of ϕ on Nu in similar to the effect of η on τ given by Fig. 8, except that the obtained curves in

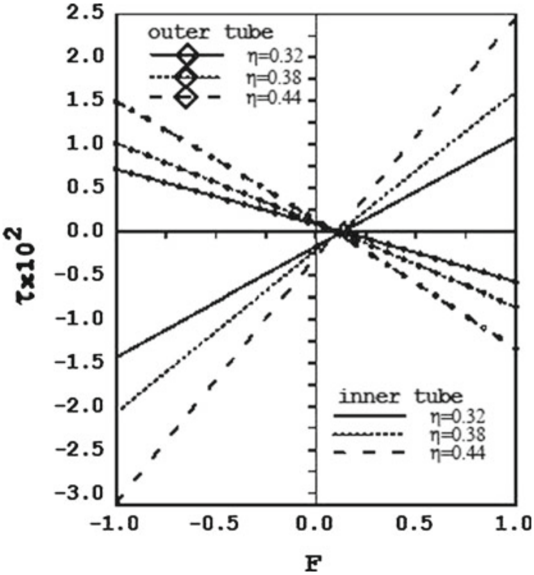

Fig. 8 The variation of τ versus F with fixed $\psi = 0.5,\ Sr = 0.6,\ E_C = 3,\ \gamma = 3,\ \lambda_1 = 0.6,\ \phi = 0.1,\ \widetilde{\varepsilon} = 0.3,\ G_C = 1,\ G_T = 1,\ n = 1.2,\ m = 1,$ and $t = 0.3$ for different values of η

this case will intersect at different points of negative Nu values which increase by increasing both ϕ and F. The effects of the Soret number Sr and the non-dimensional chemical reaction parameter γ on Nu (figures are removed) are found to be exactly similar to the effect of G_C on τ given by Fig. 7, while the effect of G_C on Nu is found to be exactly similar to the effect of η on τ given by Fig. 8, and the effect of λ_1 on Nu is found to be exactly similar to the effect of G_T on Nu given in Fig. 9. Also, the effects of η and ψ are found to be similar to the effect of η on τ given by Fig. 8 except that the obtained curves will intersect at a point of negative Nu value. Finally, the effect of the porosity parameter $\widetilde{\varepsilon}$ on Nu is found to be similar to the effect of η on τ given by Fig. 8 except that the obtained curves for small values of $\widetilde{\varepsilon}$ will not intersect, and they will be parallel lines.

The behaviors of the Nusselt number Nu as a function of time t for various values of the parameters $Sr,\ \lambda_1$, and ϕ are depicted in Figs. 11, 12, and 13, respectively, at the inner and outer tubes. Figure 11 shows that at any time $t,\ Nu$ increases (or decreases) by increasing Sr values at inner (or outer) tube, respectively, and for any value of Sr, we find by increasing t that Nu decreases (or increases) till its minimum (or maximum) value after which it increases (or decreases) at the inner (or outer) tube, respectively. Note that the increasing minimum or decreasing maximum values of Nu occur at the same time, and that the resulting curves at the inner and outer tubes respectively are symmetric about the axis $Nu = 0$. Note also that the resulting curves at high values of Sr are straight lines parallel to the horizontal axis. The effect of γ on Nu is found to be exactly similar to the effect of Sr on Nu given by Fig. 11. Figure 12 shows that at any value of $t,\ Nu$ decreases (or increases) by increasing λ_1 values at the inner (or outer) tube, respectively, and for any value of λ_1, we find by increasing t that Nu decreases (or increases) till its minimum (or maximum) value after which it increases (or decreases) at the inner (or outer) tube, respectively. Note also that for any value of λ_1, the behavior of Nu with t is similar to that obtained in Fig. 11 for any value of Sr except that the resulting curves at small values of λ_1 are straight lined parallel to the horizontal axis. The effects of $\eta,\ G_T$, and ψ on Nu are found to be exactly similar to the effect of λ_1 on Nu given by Fig. 12 except that in the later cases (effect of G_T on Nu), the resulting curves are

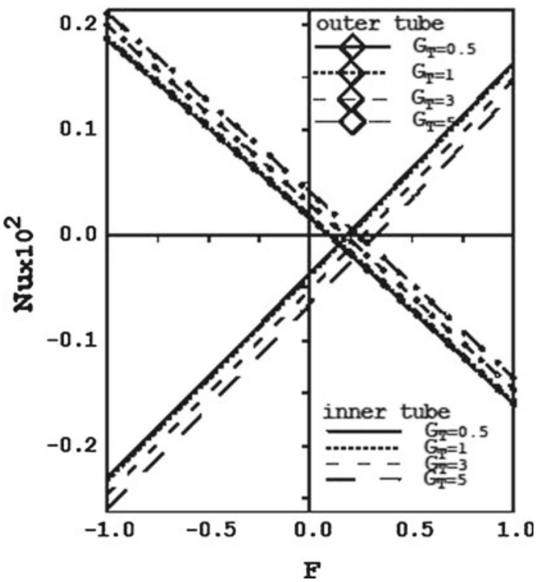

Fig. 9 The variation of Nu versus F with fixed $\psi = 0.5,\ \eta = 0.32,\ Sr = 0.6,\ E_C = 3,\ \gamma = 3,\ \lambda_1 = 0.6,\ \phi = 0.1,\ \widetilde{\varepsilon} = 0.3,\ G_C = 1,\ n = 1.5,\ m = 1$, and $t = 0.3$ for different values of G_T

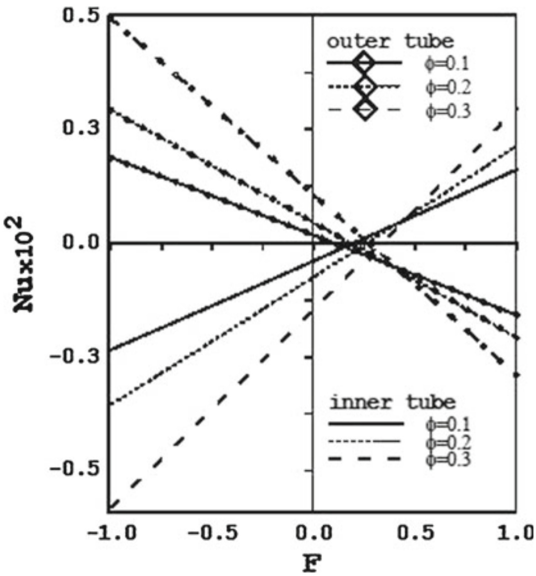

Fig. 10 The variation of Nu versus F with fixed $\psi = 0.5,\ \eta = 0.32,\ Sr = 0.6,\ E_C = 3,\ \gamma = 3,\ \lambda_1 = 0.6,\ \widetilde{\varepsilon} = 0.3,\ G_C = 1,\ G_T = 1,\ n = 1.5,\ m = 1$, and $t = 0.3$ for different values of ϕ

found to be parallel, and (effect of ψ on Nu) the resulting curves are very close to each other, while the effect of the parameters G_C and $\widetilde{\varepsilon}$ on Nu are found also to be similar to the effect of λ_1 on Nu given by Fig. 12, except that the resulting curves at small values of G_C and $\widetilde{\varepsilon}$, respectively, are straight lines parallel to the horizontal axis. The effect of the amplitude ratio ϕ on Nu is shown in Fig. 13 which indicates that its effect is similar to the effect of λ_1 on Nu given by Fig. 12 except that there are two times t_1 and t_2 ($t_1 < t_2$), where in the intervals $0 \leqslant t < t_1$ and $t > t_2$, Nu increases (or decreases) by increasing ϕ values at the inner (or outer) tube, respectively, while in the interval $t_1 \leqslant t \leqslant t_2$, Nu is found to decrease

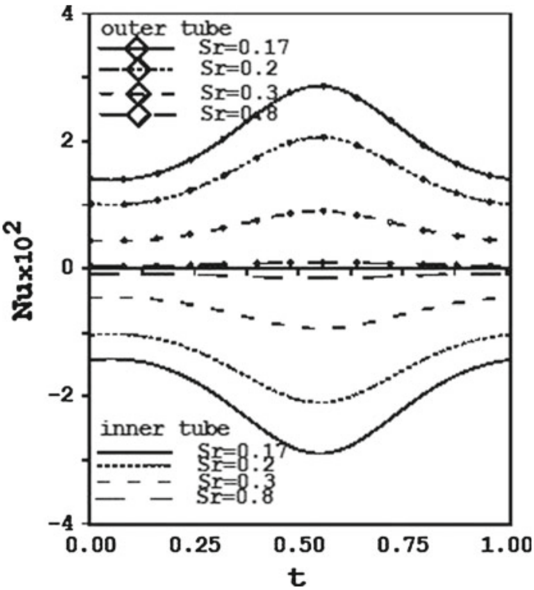

Fig. 11 The variation of Nu versus t with fixed $\psi = 0.5,\ \eta = 0.32,\ E_C = 3,\ \gamma = 3,\ \lambda_1 = 0.6,\ \phi = 0.1,\ \widetilde{\varepsilon} = 0.3,\ G_C = 1,\ G_T = 1,\ n = 1.5,\ m = 1$, and $x = 0.3$ for different values of Sr

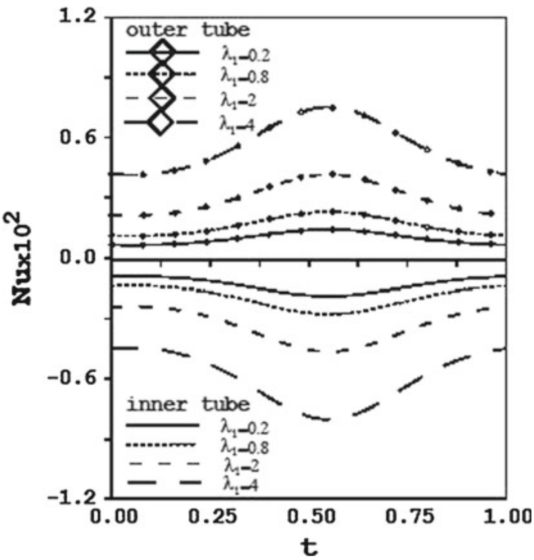

Fig. 12 The variation of Nu versus t with fixed $\psi = 0.5,\ \eta = 0.32,\ E_C = 3,\ \gamma = 3,\ Sr = 0.6,\ \phi = 0.1,\ \widetilde{\varepsilon} = 0.3,\ G_C = 1,\ G_T = 1,\ F = -1,\ n = 1.5,\ m = 1$, and $x = 0.3$ for different values of λ_1

(or increase) by increasing ϕ values at the inner (or outer) tube, respectively, and in both intervals the resulting curves will be also symmetric about the axis $Nu = 0$.

Finally, the behavior of the Sherwood number Sh as a function of time t for various values of the parameters $\eta,\ Sr,\ \phi$, and m are depicted in Figs. 14, 15, 16, and 17, respectively, at the inner and outer tubes. It is clear from Fig. 14 that at any time $t,\ Sh$ increases (or decreases) by increasing η values at the inner (or outer) tube, respectively, and for any value of η, we find by increasing t that Sh increases (or decreases) till its maximum (or minimum) value after which it decreases (or increases) at the inner (or outer) tube, respectively. Note that the increasing minimum or decreasing maximum values of η occur at the same time, and

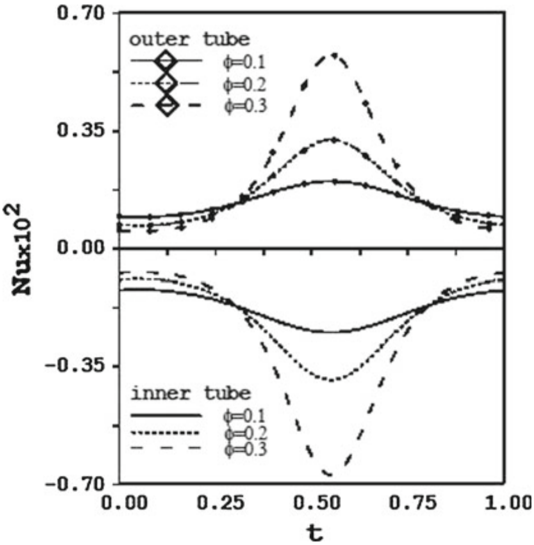

Fig. 13 The variation of Nu versus t with fixed $\psi = 0.5,\ \eta = 0.32,\ E_C = 3,\ \gamma = 3,\ \lambda_1 = 0.6,\ Sr = 0.6,\ \widetilde{\varepsilon} = 0.3,\ G_C = 1,\ G_T = 1,\ F = -1,\ n = 1.5,\ m = 1$, and $x = 0.3$ for different values of ϕ

that the resulting curves at the inner and outer tubes, respectively, are parallel and symmetric about the axis $Sh = 0$. The effect of the angle of taper ψ on Sh is exactly similar to the effect of η on Sh given by Fig. 14, except that the resulting curves in this case are very close to each other. Figure 15 shows that at any value of t, Sh decreases (or increases) by increasing Sr values at the inner (or outer) tube, respectively, and for any value of Sr, the behavior of Sh with t is similar to that obtained in Fig. 14 for any value of η. The effect of the non-dimensional chemical reaction parameter γ on Sh is found to be exactly similar to the effect of Sr on Sh given by Fig. 15. The effect of the amplitude ratio ϕ on Sh is shown in Fig. 16 which indicates that its effect is similar to the effect of η on Sh given by Fig. 14 except that there exist two times t_1 and t_2 ($t_1 < t_2$) such that in the intervals $0 \leqslant t < t_1$ and $t > t_2$, Sh decreases (or increases) by increasing ϕ values at inner (or outer) tube, respectively, while in the interval $t_1 \leqslant t \leqslant t_2$, Sh increases (or decreases) by increasing ϕ values at the inner (or outer) tube, respectively, and in both intervals, the resulting curves will also be symmetric about the axis $Sh = 0$. Figure 17 shows the behavior of Sh as a function of t for various values of the wall-concentration ratio m (positive or negative) at the inner and outer tubes. It is obvious from this figure that for any value of t, if m is positive then the value of Sh is negative and vise versa at both the inner and outer tubes. It is also obvious that Sh decreases by increasing m in both cases at the inner and outer tubes, and that the obtained curves at the inner tube is lower than the corresponding curves at the outer tube, except that the case when $m = -1$, we find that the obtained curves coincide at the inner and outer tubes. In other words, we conclude that the value of Sh at the inner tube is less than its value at the outer tube for any value of m except that when $m = -1$, at which the value of Sr is the same if the tube is inner or outer, and Sr reaches its maximum value at a definite time. Note also from Fig. 17 that for high-positive value of m, Sh has its minimum value at a definite time while for high negative value of m, Sh has its maximum value at the same time at both the inner and outer tubes.

By comparing results from this and other studies, we find that if we put $\phi = 0$ (absence of viscous dissipation) in the results obtained by Vajravelu et al. (2007) then we get the same results when we put $\psi = 0$ (uniform tube), $\lambda_1 = 0$ (Newtonian fluid), and $\gamma = 0$

Fig. 14 The variation of Sh versus t with fixed $\psi = 0.5,\ \gamma = 3,\ \phi = 0.1,\ Sr = 0.6,\ G_C = 1,\ G_T = 1,\ m = 1$, and $x = 0.3$ for different values of η

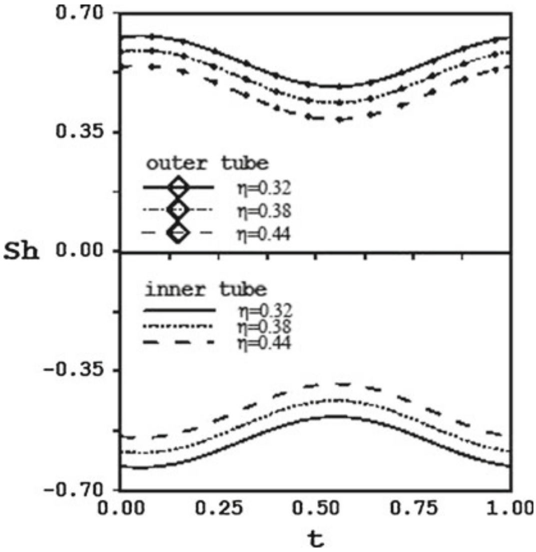

Fig. 15 The variation of Sh versus t with fixed $\psi = 0.5,\ \eta = 0.32,\ \gamma = 3,\ \phi = 0.1,\ G_C = 1,\ G_T = 1,\ m = 1$, and $x = 0.3$ for different values of Sr

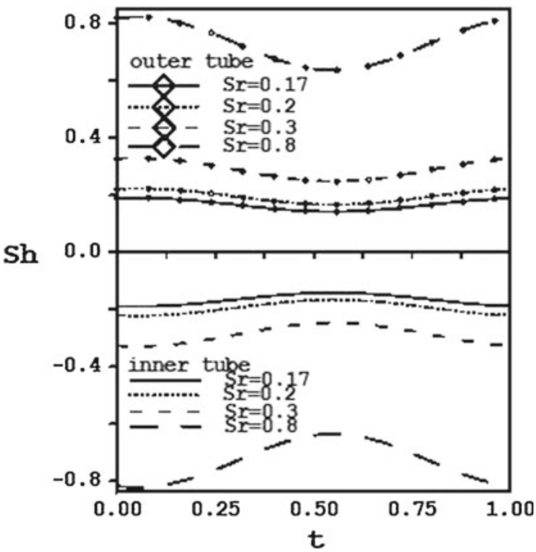

and ignore the mass transfer in this study. Moreover, we compared the results obtained by Mekheimer and Abd Elmaboud (2008) when $M = 0$ (absence magnetic parameter) and $\beta = 0$ (absence heat source/sink) then we found it agrees with the results obtained in this study for $\psi = 0,\ \lambda_1 = 0,\ \gamma = 0$ and also the effect of mass transfer on peristaltic flow has been ignored.

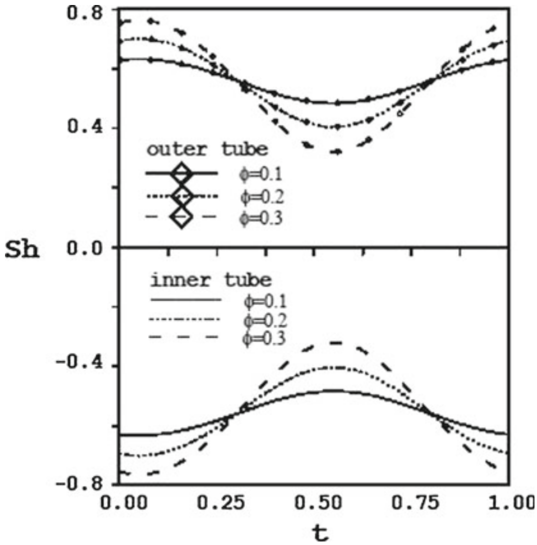

Fig. 16 The variation of Sh versus t with fixed $\psi = 0.5,\ \eta = 0.32,\ \gamma = 3,\ Sr = 0.6,\ G_C = 1,\ G_T = 1,\ m = 1$, and $x = 0.3$ for different values of ϕ

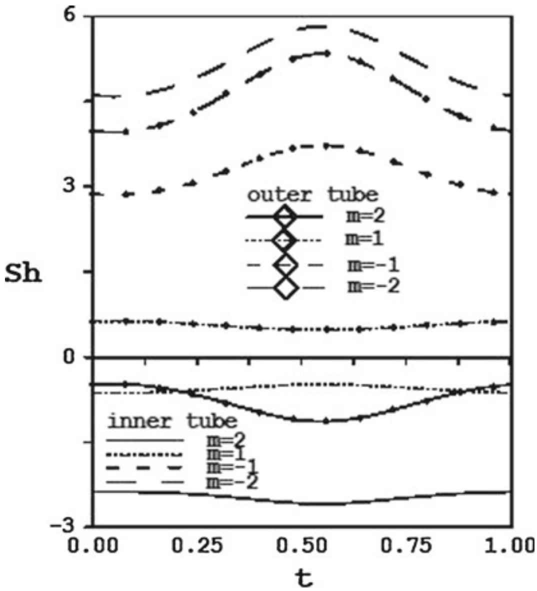

Fig. 17 The variation of Sh versus t with fixed $\psi = 0.5,\ \eta = 0.32,\ \gamma = 3,\ Sr = 0.6,\ \phi = 0.1,\ G_C = 1,\ G_T = 1$, and $x = 0.3$ for different values of m

7 Conclusions

In this article, peristaltic flow of an incompressible Jeffrey through vertical porous media in the gap between concentric tubes with heat and mass transfer in the presence of chemical reaction has been studied for the long wavelength at low Reynolds number. The outer tube is non-uniform and has a sinusoidal wave traveling down its wall, and the inner one is a rigid uniform tube. We studied the problem in 2D case using the cartesian coordinates, because it is well known that (Tang 1994; Misra and Pandey 2002) the long-wavelength asymptotic approximation in 3D case is not as good as in 2D case and also the 3D flow is more sensitive to Reynolds number change. The obtained results can be summarized as follows:

(1) The variation of the pressure rise $\Delta P_{\lambda}(t)$ as a function of the flow rate F for various values of other physical parameters indicate that in the pumping region $\Delta P_{\lambda}(t) > 0$, an increase of G_T increases the pumping rate $\Delta P_{\lambda}(t)$, and in the copumping region $\Delta P_{\lambda}(t) < 0$, the pumping rate decreases by increasing G_T. There is an inversely linear relation between F and $\Delta P_{\lambda}(t)$. The effects of the parameters $\psi,\ \phi,\ \eta,\ E_C$, and $\widetilde{\varepsilon}$ on $\Delta P_{\lambda}(t)$ and F are similar to the effect of G_T on $\Delta P_{\lambda}(t)$ and F. In the region $-1 \leq F < 0,\ \Delta P_{\lambda}(t)$ decreases by increasing λ_1, while in the region $0 \leq F \leq 1,\ \Delta P_{\lambda}(t)$ increases by increasing λ_1. Similar results can be obtained for the effect of G_C on $\Delta P_{\lambda}(t)$ and F. The effects of γ and Sr on $\Delta P_{\lambda}(t)$ are similar to the effect of λ_1 on $\Delta P_{\lambda}(t)$.

(2) The variations of the outer and inner friction forces on $F_{\lambda}^{(0)}(t)$ and $F_{\lambda}^{(i)}(t)$ appear at the outer and inner surfaces of the tubes, respectively, as a function of the flow rate F for various values of other physical parameters indicate that the outer friction $F_{\lambda}^{(0)}(t)$ has a greater value (positive or negative) than the inner friction $F_{\lambda}^{(i)}(t)$. The effects of $G_T,\ \psi,\ \phi,\ \lambda_1,\ \widetilde{\varepsilon},\ Sr,\ \gamma,\ E_C,\ G_C$, and η on any of $F_{\lambda}^{(\mathrm{o})}(t)$ or $F_{\lambda}^{(\mathrm{i})}(t)$ can be considered to have similar effects of these parameters on pressure rise $\Delta P_{\lambda}(t)$ but with a reflection about the horizontal axis F passing through the origin.

(3) The variation of the skin friction τ at the inner and outer tubes with the flow rate F for various values of other physical parameters indicate that τ decreases and increases by increasing G_C when $\tau \lesseqgtr 0$, respectively; while for any value of $G_C,\ \tau$ increases and decreases by increasing the flow rate F at the inner or outer tubes, respectively. The effects of the parameters $Sr,\ \gamma$, and λ_1 on the skin friction τ are found to be similar to the previous effect of G_C on τ. Also, the effects of other parameters as $E_C,\ G_T,\ \widetilde{\varepsilon},\ \psi$, and ϕ on τ are found to be similar to the foregoing effect of η on τ.

(4) The variation of the Nusselt number Nu at the inner and outer tubes with the flow rate F for various values of other physical parameters indicate that the resulting curves in this case will be similar to the effect of G_C on τ except that they will intersect at different points of negative Nu values which increase by increasing each of G_T and F. The effect of λ_1 on Nu is found to be exactly similar to the effect of G_T on Nu. The effects of Sr and γ on Nu are similar to the effect G_C on τ; while the effects of $G_C,\ \eta,\ \widetilde{\varepsilon},\ \phi$, and ψ on Nu are similar to the effect of η on τ.

(5) The variation of the Nusselt number Nu at the inner and outer tubes with the time t for various values of other physical parameters indicate that Nu increases (or decreases) by increasing Sr values at the inner (or outer) tube, respectively. The effect of λ_1 on Nu is opposite to the effect of Sr on Nu. The effect of γ on Nu is exactly similar to the effect of Sr on Nu. The effect of η on Nu is similar to the effects of $\lambda_1,\ G_T, and\ \psi$ on Nu. The effect of ϕ on Nu is similar to the effect of λ_1 on Nu.

(6) The variation of the Sherwood number Sh at the inner and outer tubes as a function of time t for other physical parameters indicate that Sh increases (or decreases) by increasing η values at the inner (or outer) tube, respectively. The effects of ψ and ϕ on Sh are similar to the effect of η on Sh. Also, Sh decreases (or increases) by increasing Sh values at the inner (or outer) tube, respectively. The effect of γ on Sh is exactly similar to the effect of Sr on Sh. Finally, Sh decreases by increasing m at the inner and outer tubes.

8 Appendix

The constants appear in the Eqs. 45, 48, 50, 53, and 56 are given by the following forms

$$b_1 = (1+\lambda_1)\left[\frac{G_T}{2}\left(\frac{c_1}{3}y_1^3 + c_2 y_1^2\right) + \frac{G_C}{a^2}\Phi_0^{(1)}\right]$$

$$b_2 = (1+\lambda_1)\left[\frac{G_T}{2}\left(\frac{c_1}{3}y_2^3 + c_2 y_2^2\right) + \frac{G_C}{a^2}\Phi_0^{(2)}\right]$$

$$b_3 = \frac{b_1 - b_2}{y_1 - y_2}, \quad b_4 = \frac{b_1 - b_2}{y_1 - y_2}, \quad b_5 = G_T c_1, \quad b_6 = G_T c_2$$

$$b_7 = \frac{1}{30}\left(\frac{b_3 b_5}{3} - \frac{b_6^2}{4}\right), \quad b_8 = \frac{1}{20}\left(\frac{b_4 b_5}{3} + b_3 b_6\right), \quad b_9 = \frac{1}{12}\left(b_4 b_6 - b_3^2\right)$$

$$b_{10} = \frac{4\alpha_3}{a^4}\left(\frac{2b_5}{a^2} - b_3\right), \quad b_{11} = \frac{2\alpha_3}{a^2}\left(b_4 - \frac{3b_6}{a^2}\right), \quad b_{12} = \frac{2\alpha_3}{a^2}\left(b_3 - \frac{3b_5}{a^2}\right)$$

$$b_{13} = \alpha_3^2 c_3 c_4, \quad b_{14} = \frac{1}{3}\left(\frac{\alpha_1^2}{2} + \alpha_2\right), \quad b_{15} = \frac{1}{60}\left(b_6 - \frac{\alpha_1}{3}b_5\right)$$

$$b_{16} = \frac{1}{20}\left(b_3 + \frac{\alpha_1}{2}b_6 - \frac{\alpha_2}{6}b_5\right), \quad b_{17} = \frac{1}{12}\left(b_3\alpha_1 - b_4 + \frac{\alpha_2}{2}b_6\right)$$

$$b_{18} = \frac{1}{6}\left(b_4\alpha_1 - b_3\alpha\right), \quad b_{19} = \frac{\alpha_1}{a^2}\left(\frac{6}{a^2} + \alpha_2\right), \quad b_{20} = \frac{2}{a^2}\left(\alpha_1 - 2\right)$$

$$\begin{aligned} b_{20+i^2} = E_C \Bigg\{ & -\frac{b_5^2}{2016}y_{\mathrm{i}}^8 - \frac{b_5 b_6}{252}y_{\mathrm{i}}^7 + b_7 y_{\mathrm{i}}^6 + b_8 y_{\mathrm{i}}^5 + b_9 y_{\mathrm{i}}^4 - \frac{b_3 b_4}{3}y_i^3 \\ & + \left[b_{10} + \frac{2\alpha_1}{a^4}\left(2b_6 y_i + b_5 y_i^2\right)\right]\frac{\partial \Phi_0^{(i)}}{\partial y} + \left[b_{11} + b_{12}y_i - \frac{\alpha_1}{a^2}\left(b_6 y_i^2 + \frac{b_5}{3}y_i^3\right)\right]\Phi_0^{(i)} \\ & - \left(\frac{\alpha_3}{2a}\Phi_0^{(i)}\right)^2 + b_{13}\left(\frac{1}{2a^2} - y_i^2\right)\Bigg\} \end{aligned}$$

$$b_{21+i^2} = (1+\lambda_1)^2\frac{E_C}{8}\left\{-\frac{2}{30}y_i^6 + \frac{\alpha_1}{5}y_i^5 - b_{14}y_i^4 + \frac{2}{3}\alpha_1\alpha_2 y_i^3 - \alpha_2^2 y_i^2\right\}$$

$$\begin{aligned} b_{22+i^2} = (1+\lambda_1)E_C \Bigg\{ & \frac{b_5}{252}y_i^7 + b_{15}y_i^6 - b_{16}y_i^5 + b_{17}y_i^4 + b_{18}y_i^3 - \frac{b_4}{2}\alpha_2 y_i^2 \\ & + \left[b_{19} - \frac{\alpha_3}{a^2}\left(\alpha_1 y_i - y_i^2\right)\right]\Phi_0^{(i)} + b_{20}\frac{\partial \Phi_0^{(i)}}{\partial y}\Bigg\} \end{aligned}$$

$$b_{27} = \frac{b_{24} - b_{21}}{E_C\left(y_1 - y_2\right)}, \quad b_{28} = \frac{b_{13}}{2a^2} + \frac{b_{21}y_2 - b_{24}y_1}{E_C(y_1 - y_2)}$$

$$b_{29} = \frac{8}{E_C(1+\lambda_1)^2}\frac{b_{25} - b_{22}}{y_1 - y_2}, \quad b_{30} = \frac{8}{E_C(1+\lambda_1)^2}\frac{b_{22}y_2 - b_{25}y_1}{y_1 - y_2}$$

$$b_{31} = \frac{b_{26} - b_{23}}{E_C(1+\lambda_1)(y_1 - y_2)}, \quad b_{32} = \frac{b_{23}y_2 - b_{26}y_1}{E_C(1+\lambda_1)(y_1 - y_2)}$$

$$b_{33} = \frac{1}{60}\left(b_3 b_4 - \frac{b_5}{2E_C G_T}\right), \quad b_{34} = \frac{1}{12}\left(b_{13} - \frac{b_6}{2E_C G_T}\right)$$

$$b_{35} = \frac{1}{6}\left(\frac{b_3}{E_C G_T} - b_{27}\right), \quad b_{36} = \frac{1}{2}\left(\frac{b_4}{E_C G_T} - b_{28} + \frac{b_{13}}{2a^2}\right)$$

$$b_{37} = \frac{1}{a^2}\left(\frac{14\alpha_3}{a^4}b_6 - \frac{\alpha_3}{E_C G_T} - b_{11}\right), \quad b_{38} = \frac{1}{a^2}\left(\frac{14\alpha_3}{a^4}b_5 - b_{12}\right)$$

$$b_{39} = \frac{1}{a}\left(\frac{2}{a^2}b_{12} - \frac{20\alpha_3}{a^6}b_5 - b_{10}\right), \quad b_{40} = \frac{1}{24}\left(\frac{1}{E_C G_T} - \alpha_2 b_4\right)$$

$$b_{41} = \frac{1}{6}\left(\frac{\alpha_1}{2E_C G_T} + b_{31}\right), \quad b_{42} = \frac{1}{2}\left(b_{32} - \frac{\alpha_2}{2E_C G_T}\right)$$

$$b_{43} = \frac{1}{a^2}\left(\frac{6\alpha_3}{a^4} + b_{19}\right), \quad b_{44} = \frac{1}{a^2}\left(\frac{2\alpha_1\alpha_3}{a^3} + b_{20}\right)$$

$$b_{44+i^2} = E_C G_T \frac{(1+\lambda_1)^3}{16}\left\{\frac{1}{420}y_i^8 - \frac{\alpha_1}{105}y_i^7 + \frac{b_{15}}{15}y_i^6 - \frac{\alpha_1\alpha_2}{15}y_i^5 + \frac{\alpha_2^2}{6}y_i^4 - \frac{b_{29}}{3}y_i^3 - b_{30}y_i^2\right\}$$

$$b_{45+i^2} = E_C G_T (1+\lambda_1)^2\left\{-\frac{b_5}{18144}y_i^9 - \frac{b_{15}}{56}y_i^8 + \frac{b_{16}}{42}y_i^7 - \frac{b_{17}}{30}y_i^6 - \frac{b_{18}}{20}y_i^5 - b_{41}y_i^3 - b_{42}y_i^2 - \left(b_{43} - \frac{\alpha_1\alpha_3}{a^4}y_i + \frac{\alpha_3}{a^4}y_i^2\right)\Phi_0^{(i)} - \left(b_{44} - \frac{4\alpha_3}{a^6}y_i\right)\frac{\partial\Phi_0^{(i)}}{\partial y}\right\}$$

$$b_{46+i^2} = E_C G_T (1+\lambda_1)\left\{-\frac{b_5^2}{181440}y_i^{10} + \frac{b_5 b_6}{18144}y_i^9 - \frac{b_7}{56}y_i^8 - \frac{b_8}{42}y_i^7 - \frac{b_9}{30}y_i^6 + b_{33}y_i^5 + b_{34}y_i^4 + b_{35}y_i^3 + b_{36}y_i^2 + \left[b_{37} + b_{38}y_i + \frac{\alpha_3}{a^4}b_6 y_i^2 + \frac{\alpha_3}{3a^4}b_5 y_i^3\right]\Phi_0^{(i)} + \left[b_{39} - \frac{8\alpha_3}{a^6}b_6 y_i - \frac{4\alpha_3}{a^6}b_5 y_i^2\right]\frac{\partial\Phi_0^{(i)}}{\partial y} + \left(\frac{\alpha_3}{4a^2}\Phi_0^{(i)}\right)^2 - \frac{b_{13}}{8a^4}\right\}$$

$$b_{51} = \frac{16}{E_C G_T(1+\lambda_1)^3}\frac{b_{48} - b_{45}}{y_1 - y_2}, \quad b_{52} = \frac{16}{E_C G_T(1+\lambda_1)^3}\frac{b_{45}y_2 - b_{48}y_1}{y_1 - y_2}$$

$$b_{53} = \frac{1}{E_C G_T(1+\lambda_1)^2}\frac{b_{49} - b_{46}}{y_1 - y_2}, \quad b_{54} = \frac{1}{E_C G_T(1+\lambda_1)^2}\frac{b_{46}y_2 - b_{49}y_1}{y_1 - y_2}$$

$$b_{55} = \frac{1}{E_C G_T(1+\lambda_1)}\frac{b_{50} - b_{47}}{y_1 - y_2}$$

$$b_{56} = \frac{1}{E_C G_T(1+\lambda_1)}\frac{b_{47}y_2 - b_{50}y_1}{y_1 - y_2} - \frac{b_{13}}{8a^4}$$

$$b_{57} = b_{44} + \frac{\alpha_1\alpha_3}{a^6}, \quad b_{58} = \frac{1}{a^2}\left(b_{43} + \frac{6\alpha_3}{a^6}\right), \quad b_{59} = b_{56} + \frac{b_{13}}{8a^4}$$

$$b_{60} = b_{34} - \frac{1}{a^2}\left(b_{38} + \frac{10\alpha_3}{a^6}b_5\right)$$

$$b_{61} = \frac{1}{a^2}\left(b_{37} + \frac{10\alpha_3}{a^6}b_6\right), \quad b_{62} = b_{34} - b_{60}$$

References

Abd El Naby, A.H., El Misery, A.M.: Effects of an endoscope and generalized Newtonian on peristaltic motion. Appl. Math. Comput. **128**, 19–35 (2002)

Chamkha, A.J., Khaled, A.A.: Similarity solutions for hydromagnetic mixed convection heat and mass transfer for Hiemenz flow through porous media. Int. J. Numer. Methods Heat Fluid Flow **10**, 94–115 (2000)

Chaturani, P., Pralhad, R.: Blood flow in tapered tubes with biorheological applications. Biorheology **22**, 303–314 (1985)

Chaturani, P., Samy, R.P.: A study of non-Newtonian aspects of blood flow through stenosed arteries and its applications in arterial diseases. Biorheology **22**, 521–531 (1985)

Chien, S.: Hemorheology in clinical medicine. Rec. Adv. Cardiovasc. Dis. (Suppl.) **2**, 21–26 (1981)

Cotton, P.B., Williams, C.B.: Practical Gastrointesinal Endoscopy, 3rd Ed. Oxford University Press, London (1990)

Deshikachar, K.S., Rao, A.R.: Effect of a magnetic field on the flow and blood oxygenation in channels of variable cross-section. Int. J. Eng. Sci. **23**, 1121–1133 (1985)

Dwivedi, A.P., Pal, T.S., Rakesh, L.: Micropolar fluid model for blood flow through a small tapered tube. Indian J. Technol. **20**, 295–299 (1982)

Eldabe, N.T.M., El-Sayed, M.F., Ghaly, A.Y., Sayed, H.M.: Peristaltically induced transport of a MHD biviscosity fluid in a non-uniform tube. Physica A **383**, 253–266 (2007)

Ellis, T.M.R., Phillips, I.R., Lahey, T.M.: Fortran 90 Programing (International Computer Science Series). Addison-Wesley, New York (1994)

El Misery, A.M., Abd El Naby, A.H., El Nagar, A.H.: Effects of a fluid with variable viscosity and an endoscope on peristaltic motion. J. Phys. Soc. Jpn. **72**, 89–93 (2003)

Elshehawey, E.F., El Misery, A.M., AbdEl Naby, A.H.: Peristaltic motion of generalized Newtonian fluid in a non-uniform channel. J. Phys. Soc. Jpn. **67**, 434–440 (1998)

Elshehawey, E.F., El Saman, A.R., El Shahed, M., Dagher, M.: Peristaltic transport of a compressible viscous liquid throgh a tapered pore. Appl. Math. Comput. **169**, 526–543 (2005)

Gorla, R.S.R., Bakier, A.Y., Byrd, L.: Effects of thermal dispersion and stratification on combined convection on a vertical surface embedded in a porous medium. Transp. Porous Media **25**, 275–282 (1996)

Gupta, B.B., Seshadri, V.: Peristaltic pumping in non-uniform tubes. J. Biomech. **9**, 105–109 (1976)

Hassanien, I.A., Bakier, A.Y., Gorla, R.S.R.: Effect of thermal dispersion and stratification on non-darcy mixed convection from a vertical plate in a porous medium. Heat Mass Transf. **34**, 209–212 (1998)

Hayat, T., Ali, N., Asghar, S., Siddiqui, A.M.: Exact peristaltic flow in tubes with an endoscope. Appl. Math. Comput. **182**, 359–368 (2006)

Hayat, T., Ahmad, N., Ali, N.: Effects of an endoscope and magnetic field on the peristalsis involving Jeffrey fluid. Commun. Nonlinear Sci. Numer. Simul. **13**, 1581–1591 (2008)

Hayat, T., Javed, M., Ali, N.: MHD peristaltic transport of a Jeffery fluid in a channel with compliant walls and porous space. Transp. Porous Media **74**, 259–274 (2008)

Hayat, T., Qureshi, M.U., Hussain, Q.: Effect of heat transfer on the peristaltic flow of an electrically conducting fluid in a porous space. Appl. Math. Model. **33**, 1862–1873 (2009)

How, T.V., Black, R.A.: Pressure losses in non-Newtonian flow through rigid wall tapered tubes. Biorheology **24**, 337–351 (1987)

Liao, S.J., Pop, I.: Explicit analytic solution for similarity boundary-layer equations. Int. J. Heat Mass Transf. **47**, 75–85 (2004)

Massey, B.S.: Mechanics of Fluids, 6th Ed. T. J. Press Ltd., Cornwall (1989)

Mekheimer, Kh.S.: Peristaltic flow of blood under effect of a magnetic field in a non-uniform channels. Appl. Math. Comput. **153**, 763–777 (2004)

Mekheimer, Kh.S.: Peristaltic transport of a Newtonian fluid through a uniform and non uniform annulus. Arab. J. Sci. Eng. **30**, 69–83 (2005)

Mekheimer, Kh.S., Abd Elmaboud, Y.: The influence of heat transfer and magnetic field on peristaltic transport of a Newtonian fluid in a vertical annulus: application of an endoscope. Phys. Lett. A **372**, 1657–1665 (2008)

Misra, J.C., Pandey, S.K.: Peristaltic transport in a tapered tube. Math. Comput. Model. Eng. **22**, 137–151 (1995)

Misra, J.C., Pandey, S.K.: Peristaltic transport of blood in small vessels: study of a mathematical model. Comput. Math. Appl. **43**, 1183–1193 (2002)
Nakayama, A., Koyama, H.: Free convection heat transfer over a non-isothermal body of arbitrary shape embedded in a fluid saturated porous media. Trans. ASME J. Heat Transf. **109**, 125–130 (1987)
Nakayama, A., Koyama, H.: Effect of thermal stratification on free convection within a porous medium. J. Thermophys. Heat Transf. **1**, 282–285 (1987)
Radhakrishnamacharya, G., Radhakrishnamurty, V.: Heat transfer to peristaltic transport in a non-uniform channel. Def. Sci. J. **43**, 275–280 (1993)
Radhakrishnamacharya, G., Srinivasulu, Ch.: Influence of wall properties on peristaltic transport with heat transfer. Comptes Rendus Mecanique **335**, 369–373 (2007)
Rao, A.R., Deshikachar, K.S.: MHD oscillatory flow of blood through channels of variable cross section. Int. J. Eng. Sci. **24**, 1615–1628 (1986)
Sankar, D.S., Hemalatha, K.: Pulsatile flow of Herschel–Bulkley fluid through stenosed arteries—a mathematical model. Int. J. Non-Linear Mech. **41**, 979–990 (2006)
Sankar, D.S., Hemalatha, K.: Pulsatile flow of Herschel–Bulkley fluid through catheterized arteries—a mathematical model. Appl. Math. Model. **31**, 1497–1517 (2007a)
Sankar, D.S., Hemalatha, K.: A non-Newtonian fluid model for blood flow through a catheterized artery—steady flow. Appl. Math. Model. **31**, 1847–1864 (2007b)
Sankar, D.S., Hemalatha, K.: Non-linear mathematical models for blood flow through tapered tubes. Appl. Math. Comput. **188**, 567–582 (2007c)
Shapiro, A.H., Jaffrin, M.Y., Weinberg, S.L.: Peristaltic pumping with long wavelengths at low Reynolds numbers. J. Fluid Mech. **37**, 799–825 (1969)
Shukla, J.B., Parihar, R.S., Rao, B.R.P., Gupta, S.P.: Effects of peripheral layer viscosity on peristaltic transport of a biofluid. J. Fluid Mech. **97**, 225–237 (1980)
Srinivas, S., Gayathri, R.: Peristaltic transport of a Newtonian fluid in a vertical asymmetric channel with heat transfer and porous medium. Appl. Math. Comput. **215**, 185–196 (2009)
Srinivas, S., Kothandapani, M.: The influence of heat and mass transfer on MHD peristaltic flow through a porous space with compliant walls. Appl. Math. Comput. **213**, 197–208 (2009)
Srivastava, L.M.: Peristaltic transport of a couple stresses fluid. Rheol. Acta **25**, 638–641 (1986)
Srivastava, L.M., Srivastava, V.P.: Peristaltic transport of a two layered model of a physiological fluid. J. Biomech. **15**, 257–265 (1982)
Tang, D.: Three-dimensional numerical and asymptotic solutions for the peristaltic of a heat-conducting fluid. Acta Mech. **104**, 215–230 (1994)
Vajravelu, K., Radhakrishnamacharya, G., Radhakrishnamurty, V.: Peristaltic flow and heat transfer in a vertical porous annulus, with long wave approximation. Int. J. Non-Linear Mech. **42**, 754–759 (2007)